HEAT TRANSFER TO ROUND IMPINGING JETS FROM A FLAT PLATE

by

DEEPAK MISHRA

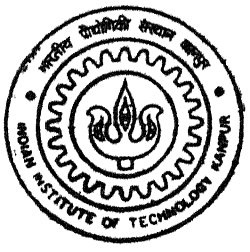

DEPARTMENT OF AEROSPACE ENGINEERING

INDIAN INSTITUTE OF TECHNOLOGY KANPUR

August, 2000

HEAT TRANSFER TO ROUND IMPINGING JETS FROM A FLAT PLATE

A Thesis Submitted
in Partial Fulfillment of the Requirements
for the Degree of

Master of Technology

by

DEEPAK MISHRA

to the

DEPARTMENT OF AEROSPACE ENGINEERING
INDIAN INSTITUTE OF TECHNOLOGY
KANPUR-208016

AUGUST 2000

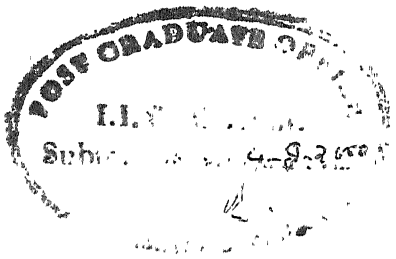

CERTIFICATE

It is certified that the work contained in the thesis entitled "Heat Transfer to Round Impinging Jets from a Flat Plate", by Mr Deepak Mishra, has been carried out under my supervision and this work has not been submitted elsewhere for a degree.

(Dr. D P. Mishra)
Department of Aerospace Engineering,
Indian Institute of Technology,
Kanpur-208016.

4th August, 2000

ACKNOWLEDGEMENTS

I express my deep sense of gratitude to my thesis advisor Dr. D.P Mishra, for his excellent guidance, invaluable suggestions, constant support and encouragement during the course of my M.Tech program. It was a great pleasure to work under him as a lot of care and personal touch was available through out.

I am thankful to Mr. V C. Shrivastav and Mr. J.B. Mishra for their help at various stages of this work. I express my appreciation and indebtedness to my friends Akilur, Sunil and Meenu who apart from helping me in this work also made my stay at Kanpur very pleasant and memorable.

Last but not the least, I am grateful to the Almighty God who gave me courage to do the job efficiently.

Deepak Mishra

Abstract

An experimental investigation of convective heat transfer to round isothermal air jets, impinging normally on a flat plate for various Reynolds numbers and nozzle-to-plate spacings has been carried out in the present work For the experimental investigation, a complete test-rig comprising of an electrically heated test plate instrumented with thermocouples and an air jet system has been designed and developed The experimental setup is validated by comparing the present data of Nusselt number with a similar kind of data available in an open literature. The present experimental results are found to be in close agreement with the results of Viskanta et al. In the present study, main attention has been focused on a square edged orifice due to its wide application in various industries An extensive series of experiments have been carried out for a square-edged orifice of outlet diameter 7 mm at Reynolds numbers 20000, 35000, 45000 and 55000 and nozzle-to-plate distances of 4, 6, 8 and 10 nozzle diameters. The local Nusselt number distribution is measured with 30-gauge iron-constantan thermocouples Average Nusselt numbers are calculated from local Nusselt numbers using the trapezoidal rule for integration Maximum stagnation point and average Nusselt numbers are obtained at separation distance of 6D and Reynolds number 55000. The subsequent highest stagnation Nusselt numbers are obtained for separation distances of 4, 8 and 10 nozzle diameters respectively at the same Reynolds number. Empirical relationships correlating the effect of variation in Reynolds numbers and nozzle to plate spacings to the Nusselt number are derived for the present data of an orifice jet. The experiments are also conducted for a convergent nozzle and a long pipe each having outlet diameter of 7 mm The results of these three configurations are compared with each other. The maximum heat transfer for pipe jets is found to be at a separation distance of 6D as in the case of orifice jets whereas, it occurs at a separation distance of 8D in the case of nozzle. It is concluded that the pipe jets produce more cooling effect at larger separation distances in the range of 6D to 8D whereas orifice jets are effective for smaller separation distances from 4D to 6D. The heat transfer in the case of nozzle jets are found to be the least among the three configurations. Only at separation distance of 8D it is higher than the heat transfer produced by orifice. An attempt for the enhancement of heat transfer to an orifice jet is also made in the present study by replacing this square-edged orifice with a sharp-edged orifice. The results obtained for two types of orifice jets are compared for Reynolds numbers 20000, 35000, 45000 and 55000 and nozzle-to-plate spacings of 4, 6, 8 and 10 nozzle diameters. This comparison shows a significant enhancement in heat transfer particularly for high Reynolds number and smaller separation distances in the range of 4D to 6D. The maximum enhancement of 18.9% in average Nusselt number is found to be at Reynolds number 55000 and separation distance of 6D.

CONTENTS

LIST OF FIGURES

List of Tables

NOMENCLATURE

Re	Reynolds number, dimensionless
Nu	Nu, dimensionless
H	nozzle to plate separation distance, mm
D	Nozzle outlet diameter, mm
q_w	wall heat flux, W / m^2
h	convective heat transfer coefficient, W / m^2-K
k	thermal conductivity of air, W / m-K
T_w	wall temperature, K
T_{aw}	adiabatic wall temperature, K
r	radial distance from the stagnation point, mm
T_∞	ambient temperature
T	temperature, K
r	radial coordinate, m
R	averaging area radius, m
T_J^0	jet total temperature, K

Subscripts

aw	adiabatic wall temperature
w	wall
0	stagnation point
j	jet or orifice at nozzle exit

Chapter 1

INTRODUCTION

1.1 Introduction

Aircraft gas turbine designers are constantly trying to increase the power output or thrust from an aero engine, reduce its weight and decrease the specific fuel consumption for a specified output. A classical way to do this is to raise the turbine entry temperature (TET) and the pressure ratio. Modern gas turbine engines are generally designed for inlet temperatures of 1400-1800 K and a pressure ratio of 20-25. The use of elevated TET and pressure ratio has significantly reduced the specific fuel consumption, size and weight of the aero engines. The only constraint that limits the rise in TET are available materials since the presently available hydrocarbon fuel can generate temperatures as high as 2000K. Over the years improvements in materials science have allowed the maximum TET to increase however at a slow rate of about 15 degrees centigrade per year but turbine designers are expected to increase the TET at a faster rate. One way of increasing this rate has been the use of turbine blade cooling which allows an increase of turbine entry temperature at a rate that is almost two times faster than the rate which improvements in materials would allow.

Turbine cooling was first considered in German designs in 1935 and after that extensively used during World War II. Convection cooling was the first method used for cooling of turbines in which the cooling air flows from the base of the blade to its end through internal passages within the blade. But this method is not adequate for the effective cooling of all parts of blade like trailing edge where concentrated cooling is required. Impingement cooling is more effective in such cases. In impingement cooling air is brought radially inside the blade through a central core and then passed through a series of holes. This air, in the form of miniature jets, is then made to impinge on the inner wall of the blade, usually just opposite from the stagnation point of the blade.

Recently a novel way has been discovered to improve the performance of a gas turbine by minimizing the gap between the ends of the blades and the shroud, reducing the leakage during the start-up or shut-down of the turbine. The gap can be minimized by

effectively controlling the temperature of the shroud and its thermal expansion with the use of impinging jets [Goldstien and Seol 1991]. The present study is inspired by the applications of impinging jets for cooling in aircraft gas turbines.

1.2 Applications

Impinging jets also find applications in many other engineering and industrial fields wherever there is requirement for rapid cooling. The areas of application where impinging air jets are used for cooling, are listed below:

1. In electronic industry, for the local cooling of hot spots on circuit boards in electronic packaging.
2. In metallurgical processing and heat treatment of some metals.
3. In the glass industry for annealing and tempering of glass.
4. A novel application of impinging jets has been discovered in the freezing of tissue in cryosurgery.

In order to study the flow and heat transfer characteristics of impinging jets, some related fundamental concepts and terminology are required and these are discussed in the next section.

1.3 Flow Characteristics of an Impinging Jet

The flow structure of an axi-symmetric jet can be characterized by dividing it into three characteristic regions - the free jet region, impinging or stagnation flow region, and the wall jet region. These three regions are depicted in the schematic of a single round jet in Figure 1.1.

In the free jet region, the shearing action of the impinging jet with ambient fluid takes place. As a result ambient air is entrained into the jet and its expansion takes place. This free jet region can be further divided into three zones: potential core zone, developing zone, and the fully developed zone, which are shown in Figure 1.2. In the potential core zone the centerline velocity of the jet remains unchanged and is equal to the velocity of the jet at nozzle exit. The length of the potential core zone depends on two factors: the velocity profile and the level of turbulence at the exit of nozzle. Generally the end of core region is defined as the point where jet velocity

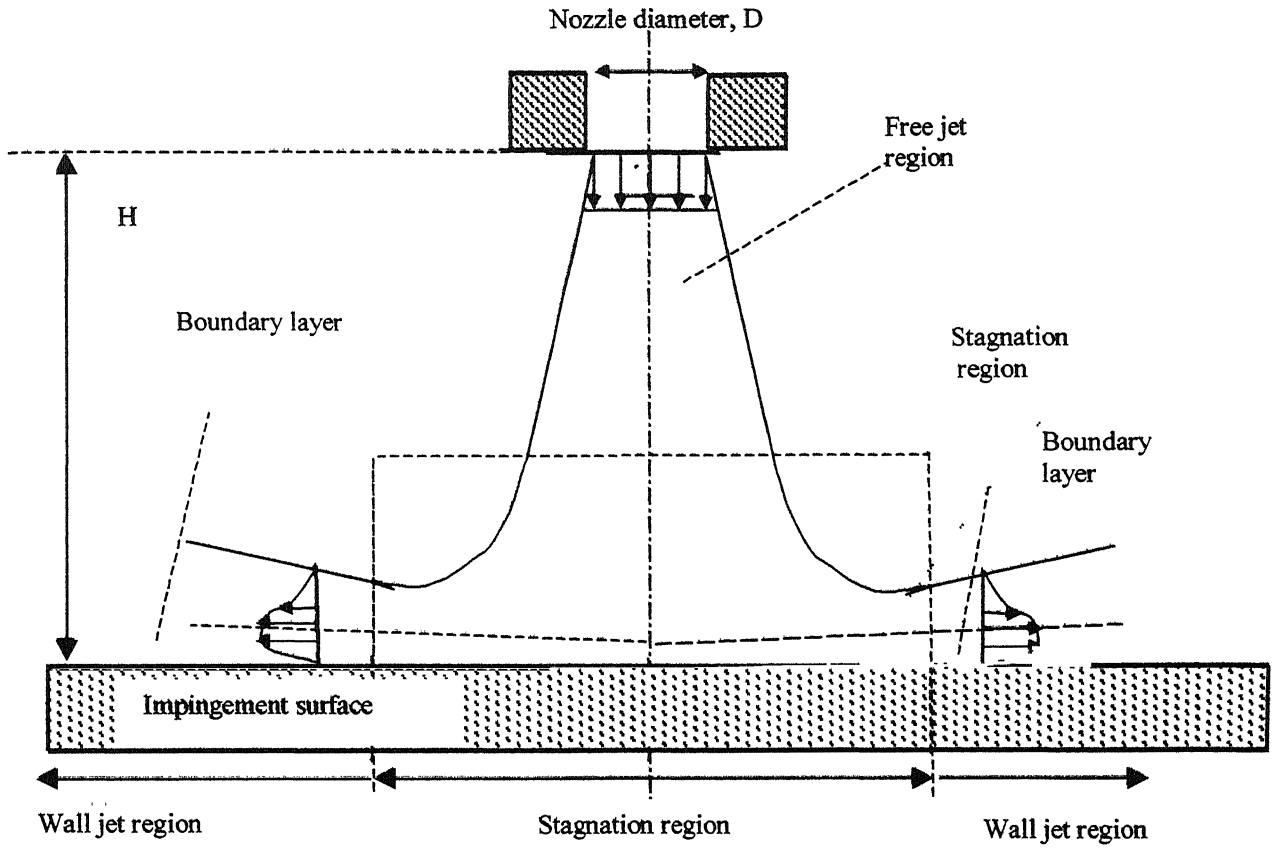

Figure 1.1 Flow regions of a free jet impinging on a flat plate

becomes 95% of the nozzle exit velocity [Gauntner et al 1970]. They proposed potential core length of 6 nozzle diameter. The developing zone is characterized by the decay of axial velocity profile of the jet due to the presence of large shear stresses at its boundary. These shear stresses generate turbulence, which subsequently give rise to the entrainment of the surrounding air into the jet stream. In the developed zone the velocity profile of the jet is fully developed. According to Reichardt [1942] a Gaussian velocity distribution best fits to the jet velocity profile found in this zone. In the stagnation zone, jet strikes the target surface and deflects in the radial direction. As a result a rapid fall in axial velocity and corresponding increase in the stagnation pressure takes place as shown in Figure 1.2. The stagnation boundary layer thickness is found to be almost constant in this region.

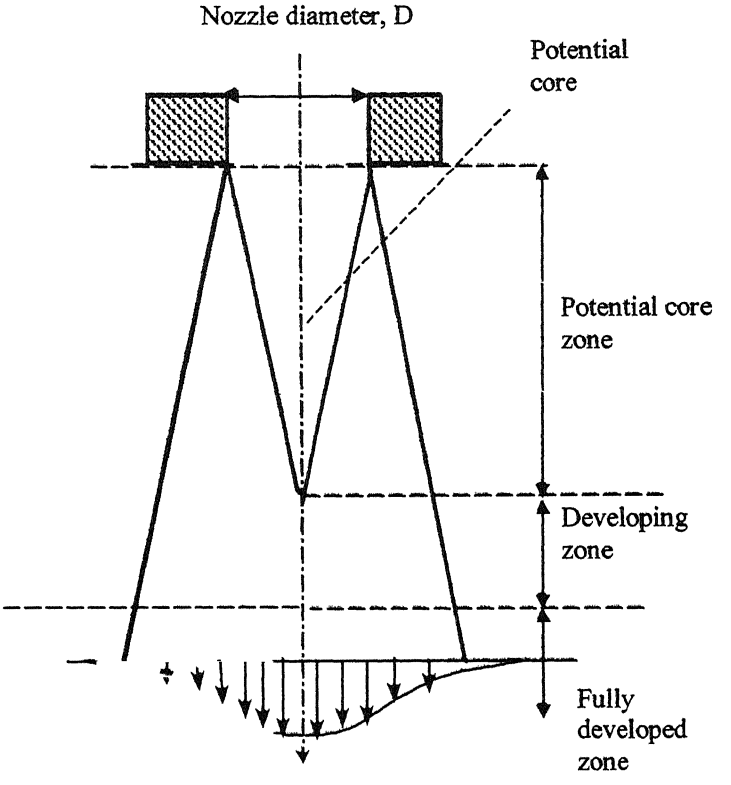

Figure 1.2 Different flow zones of a free jet

In the wall jet region the flow accelerates in the outward radial direction. The velocity is found to be maximum at approximately one jet diameter away from the stagnation point for the H/D ratio (the non-dimensional nozzle-to plate spacing) ranging from 0 to 12 [Abramovich 1963]. The wall jet region exhibits very high levels of heat transfer due to the presence of turbulence generated by the shear between the wall jet and the ambient air.

The structure of an impinging jet can be defined in terms of some geometric parameters associated with it. The basic parameters are nozzle diameter, D, and the nozzle-to-plate distance, H, which are shown in Figure 1.1 and will be used extensively in this thesis.

On the basis of Reynolds number, the impinging jets can be divided into three categories. A jet is fully laminar up to Reynolds number 1000 and becomes completely turbulent for Reynolds number higher than 3000 [Polat et al 1989]. For Reynolds

numbers ranging from 1000 to 3000, the impinging jets are considered to be in the transition state. Laminar jets are more important from the theoretical than practical point of view. The focus of discussion is on turbulent impinging jets that are used in the present study with Reynolds number ranging from 20000 to 55000.

1.4 Heat Transfer Definitions

Some important dimensionless parameters need to be defined for the present study of jet impingement heat transfer.

1.4.1 Nusselt number: It is defined as the ratio of heat flow rate by convective process to the heat flow rate by the conduction process through a layer of thickness L under a unit temperature difference.

$$Nu = \frac{q_{conv}}{q_{cond}} = \frac{h}{k/L} = \frac{hL}{k}$$

Where h is local convective heat transfer coefficient, defined as

$$h = \frac{q_w}{(T_w - T_{ref})}$$

Where q_w = convective wall heat flux

T_w = local wall temperature measured in the presence of heating

T_{ref} = reference temperature.

In the present study, the local adiabatic temperature has been used as the reference temperature. Bouchez and Goldstien [1975] showed that the heat transfer coefficient is independent of the wall heat flux if T_{aw} is used as T_{ref}. Hollworth and Gero [1985] have shown that the use of T_{aw} as T_r renders the heat transfer which is independent of the difference between the jet total temperature ($T°_j$) and ambient temperature (T_∞). By definition adiabatic wall temperature is the wall temperature in the absence of heat flux. The experimental heat transfer coefficient h and adiabatic wall temperature T_{aw}, results are presented in terms of local Nu number,

$$Nu = \frac{hD}{k}$$

Where D is the diameter of the jet.

The local Nu number distribution can be averaged to obtain a mean Nusselt number:

$$\overline{Nu} = \frac{\bar{h}D}{k} = \frac{D}{k}\int_A h\frac{(T_w - T_{aw})dA}{A\overline{\Delta T}}$$

where k = thermal conductivity of impinging fluid and the average temperature difference ΔT is defined as:

$$\overline{\Delta T} = \overline{(T_w - T_{aw})} = \int_A \frac{(T_w - T_{aw})dA}{A}$$

The mean values of both Nu and T are expected to depend on the area A over, which the quantities have been averaged. If $(T_w - T_{aw})$ is constant over the impingement surface and if the jet is axi-symmetric Eq. (5) for the mean Nusselt number reduces to:

$$\overline{Nu} = \frac{\bar{h}D}{k} = \frac{2}{R^2}\int_0^R Nu(r)rdr$$

If the heat flux $q = h(T_w - T_{aw})$, is constant over the impingement surface πR^2, the mean Nusselt number becomes

$$\overline{Nu} = \frac{\bar{h}D}{k} = \frac{qD}{k\overline{\Delta T}}$$

where

$$\overline{\Delta T_w} = \overline{(T_w - T_{aw})} = \frac{2}{R^2}\int_0^R (T_w - T_{aw})rdr$$

The jet impingement heat transfer is very complex in nature and is affected by a number of parameters like the Nusselt number, Reynolds number, Prandtl number, the non-dimensional nozzle-to-plate spacing (H/D), and the non-dimensional displacement from the stagnation point (r/D). Besides this turbulence, flow confinement, nozzle geometry, entrainment, jet outlet conditions, nozzle diameter, angle of incidence, nature of target surface, etc. are also found to be significant in the jet impingement heat transfer.

1.5 Present Investigation

The present investigation is an experimental study of impingement cooling with air jets. Three configurations are considered - orifice, nozzle, and cylindrical pipe. An attempt has also been made for an enhancement of the cooling by varying the geometry of the previously used orifice. The following studies have been undertaken as part of this work.

1. Local and average Nusselt number distributions over a wide range of non dimensional radial distance, r/D for orifice, nozzle and pipe jets at nozzle-to plate-separation distance H/D= 4, 6, 8, 10 and Reynolds number 35000. For the case of orifice, these Nu number distributions for H/D = 4,6, 8 and 10 have also been determined additionally for Reynolds number 20000, 45000 and 55000.
2. Local and average Nusselt number distribution for the sharp edged orifice at nozzle-to-plate-separation H/D=4, 6, 8, 10 and Reynolds number 20000, 35000, 45000 and 55000 and its comparison with the simple orifice for corresponding arrangements.
3. Correlation for calculating stagnation and average Nu number for various H/D ratios and Reynolds number in the case of orifice.

In the following chapter the literature available in the field of jet impingement heat transfer has been discussed in order to get the present status of the research. Subsequently, in third chapter the experimental set-up and procedure involved in this study are explained. The fourth chapter is devoted to a comparative study of orifice, nozzle and pipe jets with a section on cooling enhancement in the case of orifice jet. In the last of this chapter the whole work has been summarized and the future prospects of the work are explored.

Chapter 2

LITERATURE SURVEY

In the present chapter an extensive literature survey in the field of jet impingement heat transfer has been carried out to get familiar with the state-of-art of research and get a direction for further investigation. The two main aspects of impinging jets are found to be their flow and heat transfer characteristics. Therefore the literature available for impinging jets has been discussed under two separate sections considering these two aspects separately. In the first section studies related to the flow characteristics of the jets are considered whereas in the second section investigations made for determining heat transfer properties of impinging jets are discussed.

2.1 Flow Characteristics of a Jet

The flow properties of a jet are significant and intimately related to its heat transfer characteristics. The flow structure of the jet, velocity profile at different regions, pressure distribution and turbulence level are the properties which govern the heat transfer characteristics of an impinging jet. Many investigators in the past have made attempts to ascertain the complex nature of the impinging jets. A pioneering work characterizing the flow structure of impinging jets was presented by Schrader, Glaser and Davidzon [1962]. Their work established the first picture of jet structure dividing it into three characteristic regions of free jet flow, stagnation flow and lateral flow outside the stagnation zone. In 1954, this lateral flow region outside the stagnation zone was termed as wall jet region by Glauert, Scholtz and Trass [1970] carried out theoretical and experimental study for a laminar and non–uniform impinging jet and compared their theoretical results with the experimental investigations. The theoretically predicted velocity and pressure distribution agree with the experimental results. Schlunder [1967] presented a relation for the axial velocity calculation and determined the velocity profile at different points of the jet axis. Donaldson and Snedeker [1971] made an extensive study on free jets and put forward many relations for jet velocity profile, its decay along the axis and wall jet characteristics with pressure distribution for impinging jets. In the impingement region there is a rapid decrease in axial velocity and a corresponding rise in static pressure. The radial pressure

distribution on impingement surface strongly affects the jet heat transfer characteristics and is quite useful in establishing correlation for the Nusselt number. Giralt et al [1977] proposed a model of characterization for the impingement region and measured the pressure distribution around the impingement zone. He suggested that the height of the impingement zone is equal to 1.2 nozzle diameter.

The flow characteristics of jets are strongly related to their cooling behavior and largely affect their heat transfer characteristics. By suitable control of geometric parameters associated with jets, the effect of these characteristics like velocity profiles, the rate of decay of centerline velocity and the level of turbulence can be effectively directed to enhance the heat transfer by the impinging jets.

2.2 Heat transfer characteristics

Jet impingement cooling problem has drawn the attention of several researchers in the past few decades. However, the complex nature of impinging jets needs to be further investigated, as it is not understood completely. Friedman & Mueller [1951] were probably the first to study the heat transfer characteristics of impinging jets. They used a calorimeter to measure the heat flux but it had a poor resolving power due to its bigger size. An early work on jet impingement heat transfer was presented by Perry, who in 1954, looked at the variations of average heat transfer coefficient produced by an inclined jet. However he presented data for a limited nozzle to plate distance of 8. From his experiments he concluded that stagnation heat transfer coefficients decrease as the angle of incidence is reduced from 90 but the average heat transfer rate was found to stay nearly constant. Vickers [1959] also presented a pioneering work in this area by studying the local heat transfer coefficients of fluid jets impinging on a normal surface but only for laminar flow region in the range of Reynolds numbers 250 to 950 and nozzle to plate distances 8 D to 10D.

In 1962, Gardon and Cobonpue presented a very useful work in this area. They devised a transducer for measuring heat flux with an excellent resolution. Their Reynolds numbers were in the wide range of 7000 to 112000 and the nozzle diameter was varied from 3.175 mm to 9.0 mm. They were the first to introduce the concept of adiabatic wall temperature and proposed that the rate of heat transfer from an impinging jet is

proportional to the difference between the target plate temperature and adiabatic wall temperature. In their experiment the maximum heat transfer was found at the distance of 6 to 7 nozzle diameters. Interestingly they also observed the presence of three maximas at radial distances of 0.5, 1.4 and 2.5 nozzle diameters from stagnation point for low Reynolds and small nozzle to plate distance. Later in 1988 Popiel and Boguslawaski confirmed the presence of these maximas.

Gardon and Akfirat [1965] investigated the effect of turbulence on jet impingement heat transfer. They showed that the turbulence intensity in a free jet could reach 30 percent higher than that at exit at approximately 8 nozzle diameters downstream of the nozzle. They also suggested that due to high level of turbulence heat transfer rate might increase even beyond the end of potential core. In 1977, Holger Martin presented a broad literature survey on jet impingement heat transfer related to mainly industrial heating and drying, covering mainly larger nozzle diameter and turbulent Reynolds numbers. His literature survey has proved to be very useful in the study of jet impingement heat transfer.

For laminar and slot jets, both Scholtz and Trass [1977] and Sparrow and Lee [1975] have shown that impingement heat transfer is very sensitive to changes in the initial velocity profile at the nozzle exit. For turbulent jets, the effect of exit profile might well be expected to be significant, particularly at small values of nozzle-to-plate spacing. Hoogendoorn [1977] worked on the influence of small-scale turbulence on heat transfer by impinging jets. He showed that the level of turbulence at the nozzle exit has an impact on the stagnation point heat transfer. He found out that an increase in the level of turbulence from 0.5 to 3.2 percent (at Re = 60000 and H/D = 2) raises the Nu number from 180 to 215 at the stagnation point and eliminates the presence of local minima often seen at small nozzle to plate distance.

In 1979 Obot et al suggested that the variation in turbulence level due to different types of nozzle designs varies the optimal nozzle to plate spacing for maximum heat transfer. They compared maximum heat transfer from a sharp-edged inlet nozzle of L/D ratio 1 with a contoured inlet nozzle and found out that for sharp-edged nozzle maximum Nu number of 155 occurs at H/D = 4 whereas for contoured–shaped nozzle its value is

only 125 at H/D = 8. They concluded that the effect of nozzle geometry on stagnation region heat transfer is predominant for H/D < 6. They also found that heat transfer is less for confined jets. Yokobori et al [1980] in their experimental work investigated the influence of turbulence caused by the large eddy structures on stagnation region heat transfer of the two-dimensional jet. They conducted flow visualization and showed that vortices, known as toroidal vortices are generated by the shearing action of the jet around its circumference. They explained that these vortices impinged on the surface and help in increasing the heat transfer. Later in 1991 Popiel and Trass further explained this phenomenon and suggested that these toroidal vortices are responsible for the generation of ring-shaped eddies at the point where they collide with the target plate.

Katoaka et al in 1984, 1987,1988 studied the effect of turbulence on heat transfer rate and suggested correlation for the Nusselt number at the stagnation point. Apart from Hoogendoorn et al, they measured turbulence level at the 0.3 jet diameter upstream of the stagnation point. Katoaka showed that the heat transfer is largely affected by the large-scale eddy structures and the enhancement of stagnation point heat transfer is mainly due to the turbulent surface renewal effect by the large eddies. He suggested that the unsteady separation of laminar boundary layer takes place due to large scale eddies at the stagnation point for nozzle to plate spacing greater than 6.Their experimental data clearly shows that turbulence intensity is maximum for nozzle to plate spacing 7 and maximum stagnation point Nusselt number occurs in the range of nozzle to plate spacing 5 to 8.

Goldstein et al [1990] in their investigations studied the effect of entrainment on jet impingement heat transfer. It has been noticed that when the jet temperature becomes different from the temperature of the surroundings, fluid entrains into the jet and affects its heat transfer performance. Goldstein et al, in their experiment used a heated jet from an ASME nozzle impinging on an electrically heated flat stainless steel plate with thermocouples fixed at different locations. The effect of entrainment is characterized by recovery factor, effectiveness and Nusselt number. They concluded that the heat transfer coefficient is independent of the relative magnitude of the jet temperature and the ambient temperature provided the adiabatic wall temperature is used as a reference

temperature in the definition of heat transfer coefficient. Therefore the heat transfer coefficient for impinging jets with $T°_j = T_\infty$ which have extensively studied.

In 1996 Viskanta et al compared heat transfer rate produced by the square orifice and hyperbolic nozzles. They found that for small nozzle to plate spacing and large Reynolds numbers, local and average heat transfer rates are enhanced for properly designed hyperbolic nozzle in comparison to a square orifice.

Most of the published literature mentioned above pertains to jets generated with well-rounded convergent nozzles. However in many applications, square edged orifices are preferred because of ease of fabrication and installation. Keeping this need and importance of orifice in view, the present study is dedicated to explore the heat transfer properties of an orifice. Moreover in jet impingement cooling the role of different nozzle configuration is quite important as different nozzle configurations behave differently because of variation in their geometry. The study of their optimum behavior under different geometric arrangement is very interesting. The above literature survey shows that only a few researchers like Sparrow and Lee and Obot et al have studied the effect of nozzle configuration on the impingement heat transfer. The work of Sparrow and Lee is limited to the laminar jets. Obot et al experimented with contoured nozzle of different designs and L/D ratios. Therefore it remains to explore the performance of various types of nozzle configurations of different geometry. The orifice, the convergent nozzle, and the circular pipe are three main types of configurations used in different engineering and industrial applications. In order to study this an experimental rig for performing the tests has been designed and fabricated in the propulsion laboratory at IIT Kanpur, which will be described in detail in the next chapter.

Chapter 3

EXPERIMENTAL SET-UP AND PROCEDURES

3.1 Introduction

In this chapter a complete description of the experimental rig along with a brief account of the fabrication process involved have been presented. The methods of measurement, calibration process of the measuring instruments, and the procedure for conducting the experiment with necessary precautions, have also been discussed in detail. The experimental setup is validated by comparing it with a similar study reported in literature. The chapter has been discussed under the following headings:

1. The test facility
2. Experimental models
3. Measurement methods
4. Experimental procedure
5. Experimental precautions
6. Validation of experimental setup
7. Summary and Conclusions

3.2 The Test Facility

In order to study the jet impingement cooling, a test facility has been developed in our laboratory. A complete schematic of the jet test rig is shown in Figure 3.1. This section has been described under the following sub-headings:

1. Experimental rig
2. Air system
3. Electrical system

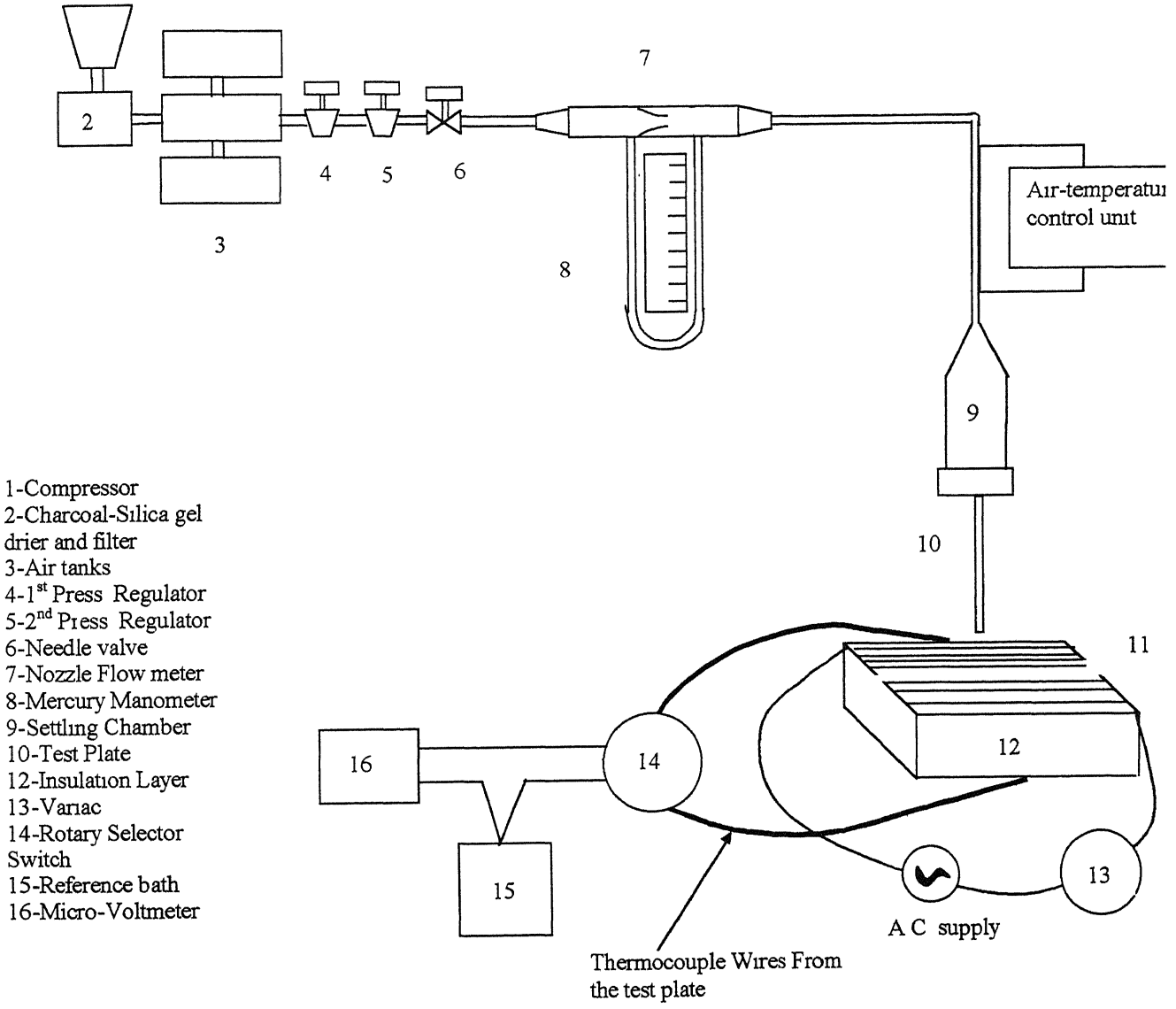

Figure 3.1 Schematic of Experimental Set-up

3.1.1 Air System

The air for conducting this series of experiments has been taken from a large storage system consisting of three vessels each of volume 90 cubic meter as shown in Fig. 3.1. The air is stored in these tanks at a pressure around 15 atm. A reciprocating compressor with a discharge of 32 m^3 per minute, driven by 150 hp electrical motor, is used to charge the storage tanks. Compressed air from the compressor is passed through a filter unit to remove the impurities and oil contamination and subsequently through electrically heated drier units containing silica gel before reaching the storage tanks.

The airflow rate is metered with the help of a nozzle flow meter, which is designed, developed and calibrated in our laboratory. Pressure regulator and needle valve controls are provided before nozzle flow meter for controlling the flow. The temperature of the air is controlled by passing it through a long (1 m) stainless steel pipe of diameter 8 mm with a heating element wound around it. The current to the temperature-controlling element is supplied by a variac. This variac gets power input through a relay, which is operated by a thermostat. When the temperature of the air falls due to expansion, this thermostat switches on the electric supply to the heating element and the air temperature starts increasing. It senses the temperature of the air by a chromel-alumel thermocouple, installed inside the settling chamber and cuts the electric power supply if the temperature of air goes above the ambient temperature. In this way the temperature of the air is maintained close around ambient temperature. The air is then entered into the settling chamber through its conical entrance. The settling chamber is shown in Figure 3.4.

The settling chamber is made of a 200-mm long cylindrical pipe of diameter 100-mm. Shields are provided to dampen the disturbances inside the settling chamber. At the exit of the settling chamber a provision has been made for fixing the different experimental models. This settling chamber is mounted on a traversing support in order to facilitate its movement for varying the nozzle to plate separation distance.

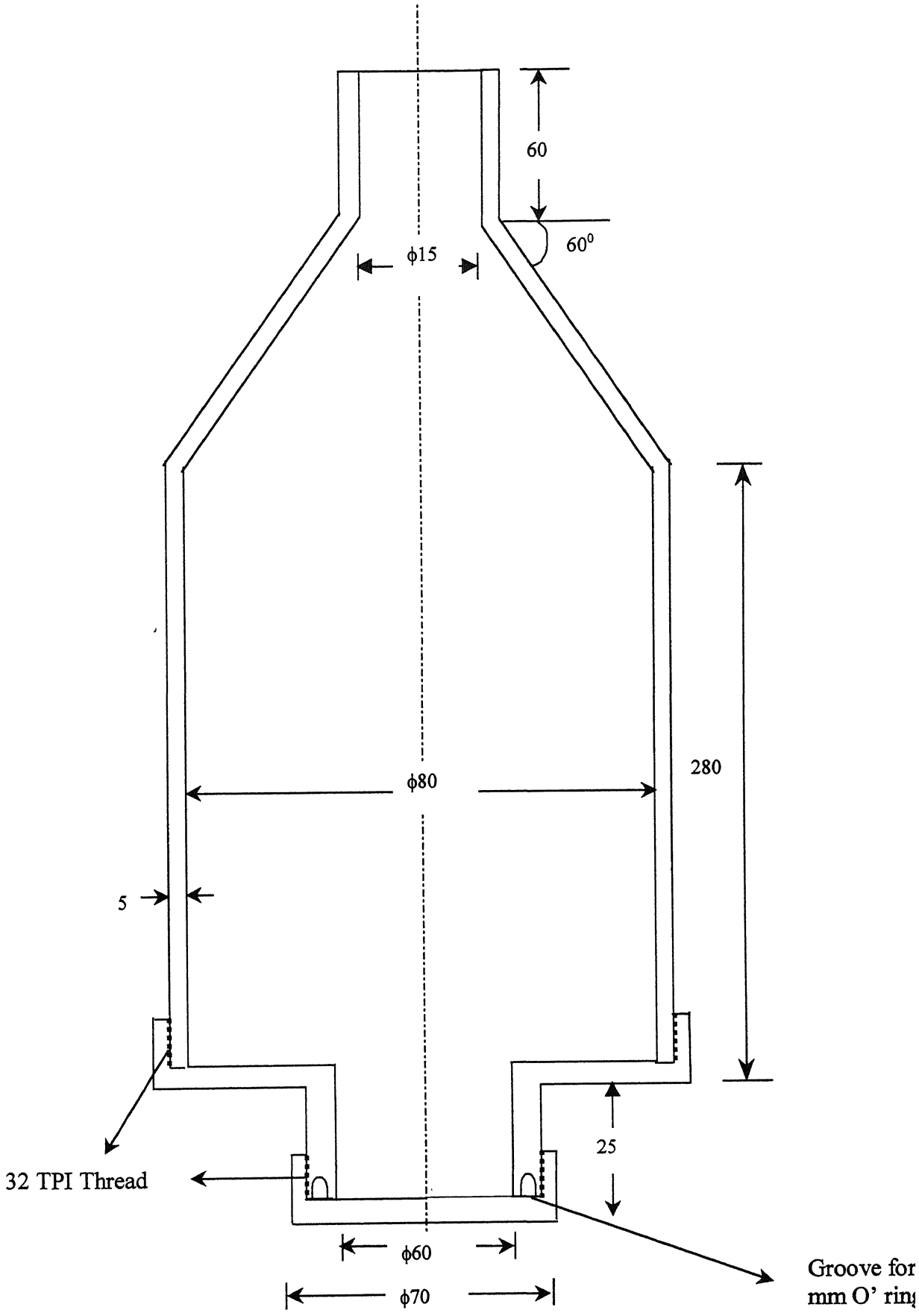

3.2 The Settling Chamber

3.1.2 The Experimental Rig

The experiments in the present study of jet impingement heat transfer are conducted on a flat test plate, which has been designed and fabricated in the laboratory. It is heated electrically in order to produce a uniform heat flux over its surface and instrumented with temperature sensors. A schematic of the test plate is shown in Figure 3.3. The upper surface of the test plate is covered with nine identical strips of stainless steel foil placed side by side. These foil strips are joined to work as a resistor and produce uniform heat flux at its surface when an electric voltage is applied across it. Each strip has a length of 280 mm with a width of 3 mm. The foil used is very thin approximately 50 μm in thickness in order to obtain good electric resistance. These strips are joined side-by-side on a 3 mm thick bakelite sheet of the size 284 x 296 mm and connected in series with the help of copper bus bars as shown in Fig. 3.3. The other side of the test plate is covered with a 50 mm thick foam insulation and a10 mm thick wooden plate for structural rigidity and to prevent heat loss from the back of the plate. With this arrangement the typical value of heat flux losses is not more than 5 W/m^2 [Goldstien et al 1984] Leveling screws are provided, in order to set the test plate in horizontal position. In the half-length of the middle foil strip twenty-nine iron-constantan thermocouples of 30-gauge wire are fixed at equal interval of 5 mm. The thermocouple ends are taken out through the insulating foam as well as wooden covering and extended further with the help of copper wires of thickness 1 mm. These extension wires are bunched together and wrapped in an aluminum foil. This aluminum foil is electrically ground in order to prevent noise from affecting the outputs of the thermocouples. The other ends of these thermocouple extension wires are connected to an OMEGA 2-pole 60-ways rotary selector switch which distributes the output of these thermocouples to a micro voltmeter of 1μV resolution.

Many difficulties were encountered while fabricating this test plate. The wrinkle free joining of thin foil on the bakelite plate was found quite difficult. A number of unsuccessful attempts were made. Finally in order to apply uniform pressure on plate surface two 10 mm thick iron plates of size 320x320 sq. mm with good surface finish were fabricated. For joining the foil on bakelite surface, an adhesive was applied on the

whole surface of bakelite plate and a stainless steel foil of equal size was placed over it. Care was taken not to allow any air pocket in between. Initially Araldite was used to make the joint but it failed at high temperature. Therefore several other adhesives were tried out and finally silicon adhesive was found to endure high temperature. After placing thin foil over bakelite sheet, it was pressed between the iron plates with the help of C-clamps and cured for one week at ambient temperature. Then with a precision milling cutter of thickness 0.3 mm, the foil bonded to the bakelite sheet was parted into nine equal strips of width 3 mm, leaving the bakelite sheet uncut. The separation between the strips was maintained at around 0.3 mm as the milling cutter used was of the same thickness. Finally these foil strips were joined in series with copper bus bars as shown in Figure 3.3.

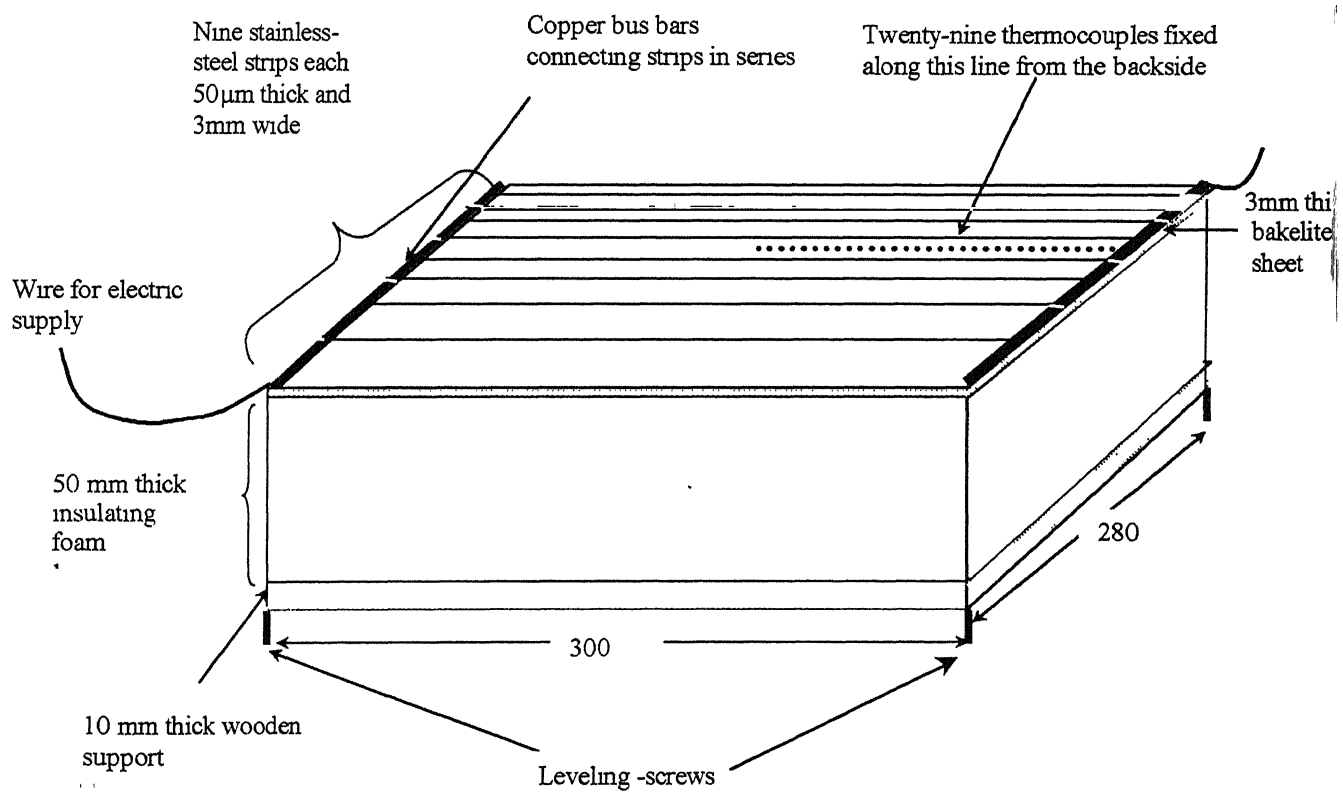

Figure 3.3 The Experimental-Rig

All Dimensions in mm

3.2.3 Electrical System

The electric power for the test plate is taken from the laboratory AC power supply. The supply is stabilized, stepped-down and subsequently controlled with a variac. A 3½ -digit ampere meter of capacity 20 amperes is connected in series with the test plate power supply. The voltage across the test plate is measured with the help of a 4½ -digit A.C. voltmeter. All connections are made with high amperage copper wires.

3.3 Experimental Models

In the present study three types of models - orifice, high area ratio convergent nozzle, and a cylindrical pipe are employed. Schematics of these models are shown in Figure 3.4. They are briefly described as follows:

The orifice used in this study is a simple circular aluminum disc of diameter 58 mm and thickness 3 mm. At its center a round straight precision hole of 7± 0.01mm diameter is made. The thickness to diameter ratio is found to be 0.444. It is designed so that it can be fixed to the lower part of the settling chamber. Another orifice with an identical round hole at its center is fabricated for enhancement study. In this orifice the central hole is chamfered at 60° to make it sharp edged. This orifice is mounted on the settling chamber with its chamfered side downwards.

The nozzle used in the present study is a convergent type nozzle with an area ratio of 16 to produce a one dimensional velocity profile at its exit. The inlet of the nozzle is round shaped with a diameter of 30 mm. Its outlet is a rounded hole of diameter 7± 0.01 mm. On the inlet side of the nozzle a flange has been provided to facilitate its fixing to the end of the settling chamber.

The third type of model used in the present study is a simple circular seamless stainless steel pipe of the inner diameter 7±0.01 mm. The outer diameter of the pipe is 10 mm. The length of the pipe is taken as 70 mm in order to allow the flow to develop fully at the exit. At the end of the pipe a disc is provided for its fixing at the exit of settling chamber. Enough care is taken to keep outlet diameters equal for all three configurations, used in the present work.

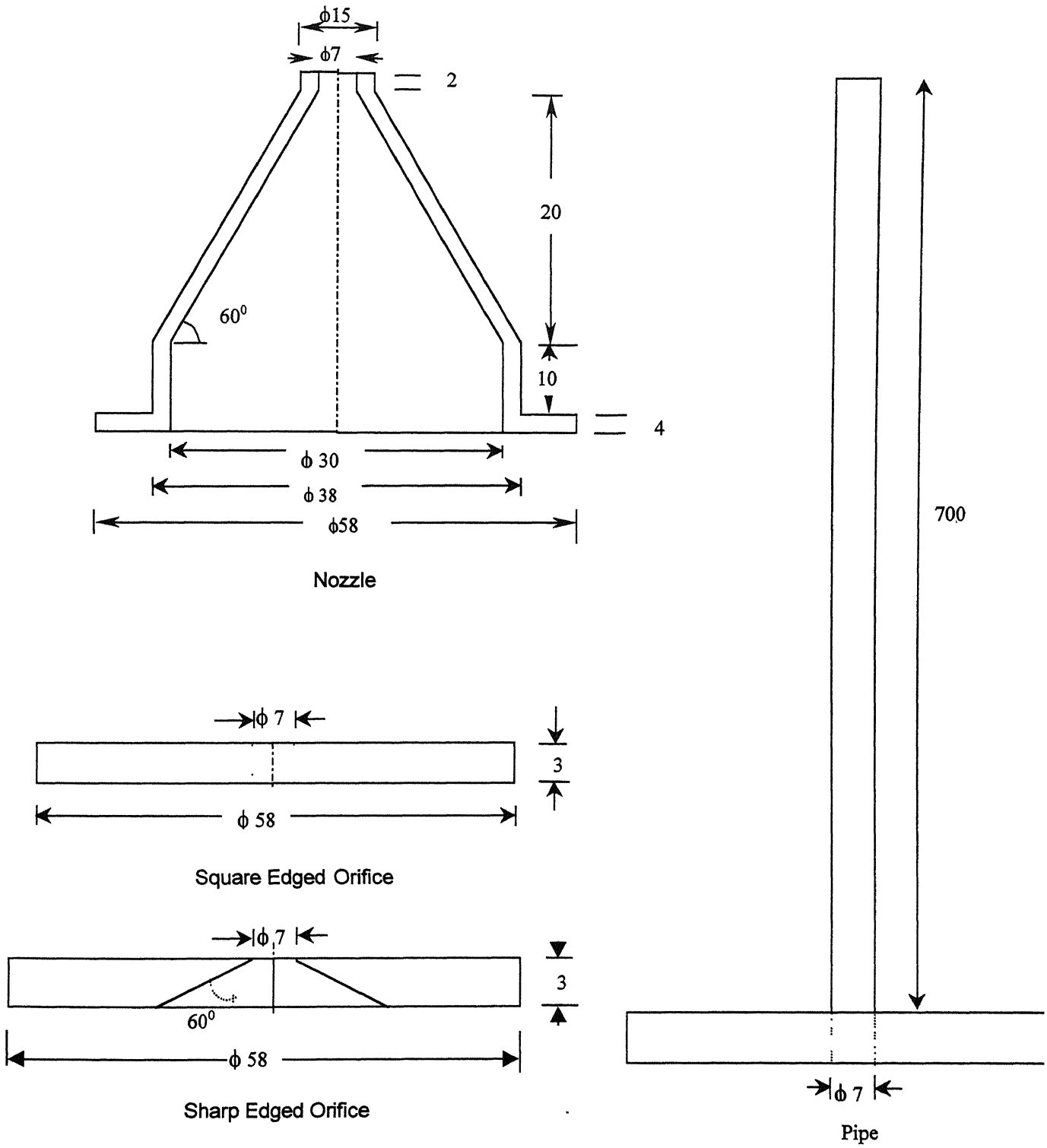

Figure 3.4 The Experimental Models

3.4 Measurement Methods

3.4.1 Airflow Measurement

The airflow was measured with the help of a nozzle flow meter, which is described below:

3.4.1.1 Nozzle Flow Meter

In our experiment a nozzle flow meter is employed to measure the airflow rate. Its nozzle is designed as per ASME code with an outlet diameter of 6±0.01 mm. It is fixed between the flanged ends of two stainless steel pipes of equal internal diameter of 26.0 mm. Pressures ports are located at D and D/2 distance from the nozzle in the upstream and downstream directions respectively. The length of the upstream pipe is taken 1 meter in order to ensure the fully developed flow just before the flow obstructing nozzle. The nozzle meter is provided conical adapters at ends for the smooth flow of air at its entrance and exit. Subsequently, this flow meter is calibrated with the help of a Pitot-static tube as explained below.

3.4.1.2 Calibration of Nozzle Flow Meter

A schematic diagram of the calibration setup for the nozzle flow meter is shown in Figure 3.6. For the calibration purpose a specially fabricated nozzle of diameter 5±0.01 mm is employed. It is fixed at the exit of flow meter in order to obtain one-dimensional velocity profile. This nozzle also helps in increasing the exit velocity of the flow in order to produce substantial manometric head. The schematic of this calibration nozzle has been shown in Figure 3.5. A Pitot-static probe is employed to measure the dynamic head associated with the flow at the exit of the nozzle. The Pitot tube is connected to a mercury manometer and aligned properly with the direction of flow at the exit. A water tube manometer of arm length 2 m is employed to measure the differential pressure across the pressure ports of flow meter. Then the air is allowed to flow through the flow meter and water level in the manometer is set at a fixed value. The corresponding reading of the mercury manometer is noted carefully. With the help of the mercury head produced, the jet exit velocity is calculated.

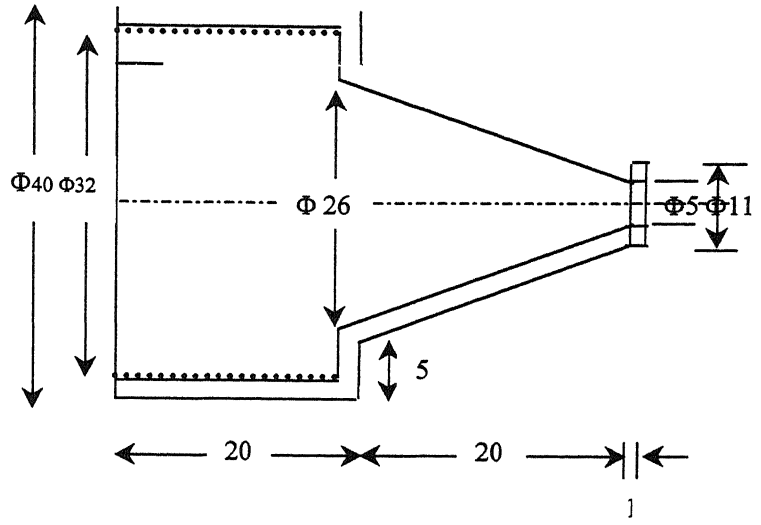

Figure 3.5 Nozzle for the Calibration of Flowmeter

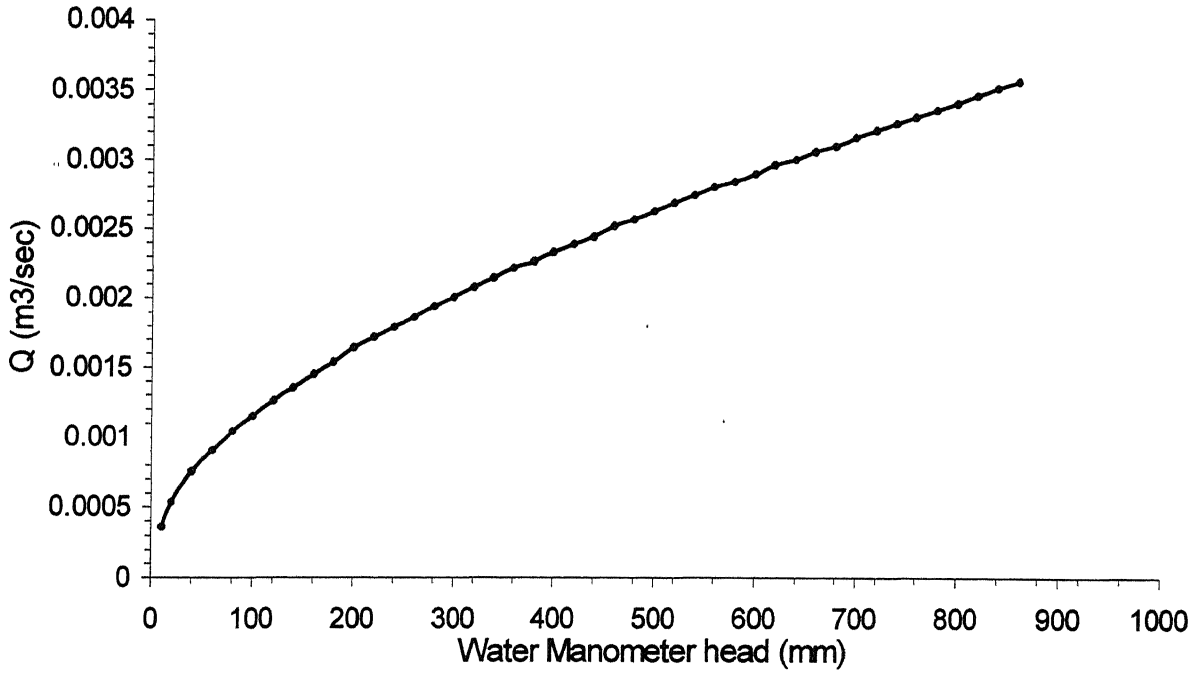

Figure 3.6 Calibration Chart for Nozzle Flow Meter

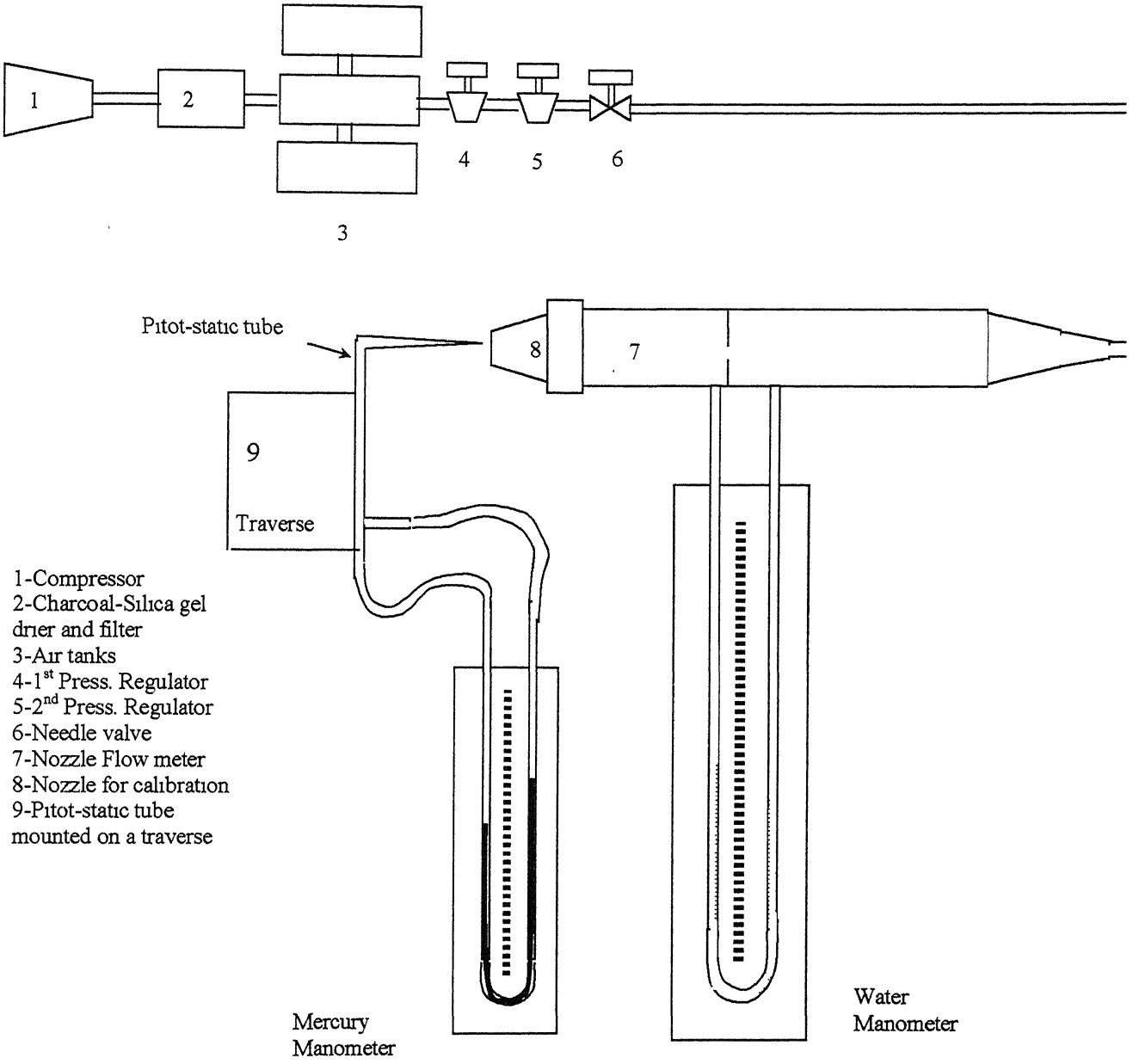

Figure 3.7 Calibration set Up for Nozzle Flow Meter

Since the jet has flat velocity profile, the flow rate can be calculated as the product of nozzle exit area and the jet exit velocity. Similar runs are made for different values of manometric head in the water manometer. A calibration curve is plotted between the flow rate of air and the corresponding water head across the pressure ports, which has been shown in the Figure 3.6.

3.4.2 Temperature Measurement

Temperature distribution produced by the cooling jet on the surface of the test plate is determined with the help of iron-constantan thermocouples. These thermocouples are calibrated for precision measurement of the temperature. For this purpose, a calibration unit is designed and developed in our laboratory, which is shown in Figure 3.8 It is basically a double walled cylindrical container of 5 liters and is filled to the top with vegetable oil. Insulating material is packed between the two walls of the container to prevent the heat loss. An immersion heating element is also installed inside the container in order to heat the oil. The current to the heater is through a relay which is actuated by a contact thermometer. All these units work together to maintain the oil temperature almost constant. In order to calibrate a thermocouple, it is dipped in the oil-bath of the calibrator unit and the oil is maintained at a particular temperature. An electrically powered stirrer dipped inside the oil-bath keeps the oil temperature uniform. The ends of this thermocouple are joined to the reference iron-constantan thermocouple that is dipped in another oil bath. A micro-voltmeter of resolution 1 microvolt is connected in series to this thermocouple circuit. The temperatures of both the oil baths are recorded with the help of standard mercury thermometers. The millivolts produced corresponding to the temperature difference between the two baths are recorded. Similar runs are made for different temperature settings of the oil bath and a calibration curve is plotted between the millivolts produced and the temperature difference. This calibration curve has been shown in the Figure 3.9.The temperature data is compared with the standard data provided by Omega. The error encountered during the measurement of different temperatures is shown in Figure 3.10.

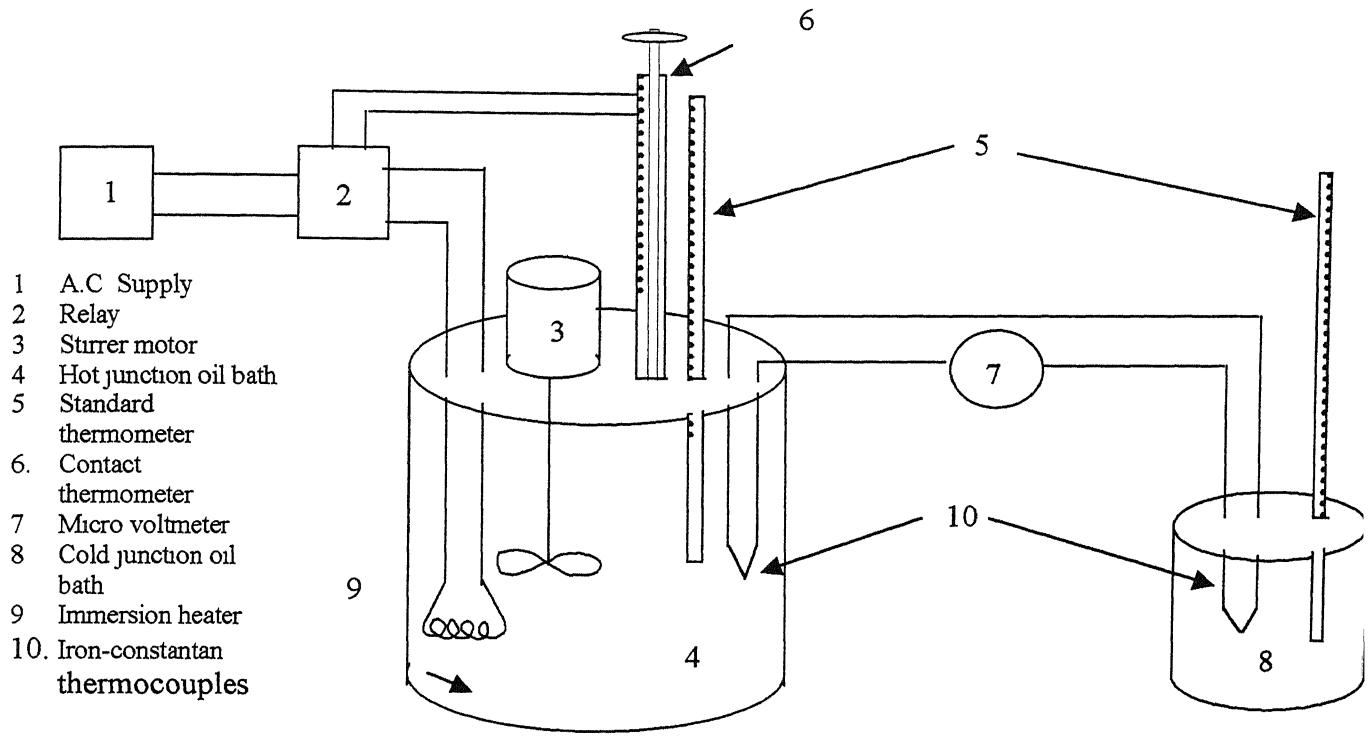

Figure 3.8 Setup for the Calibration of Thermocouple

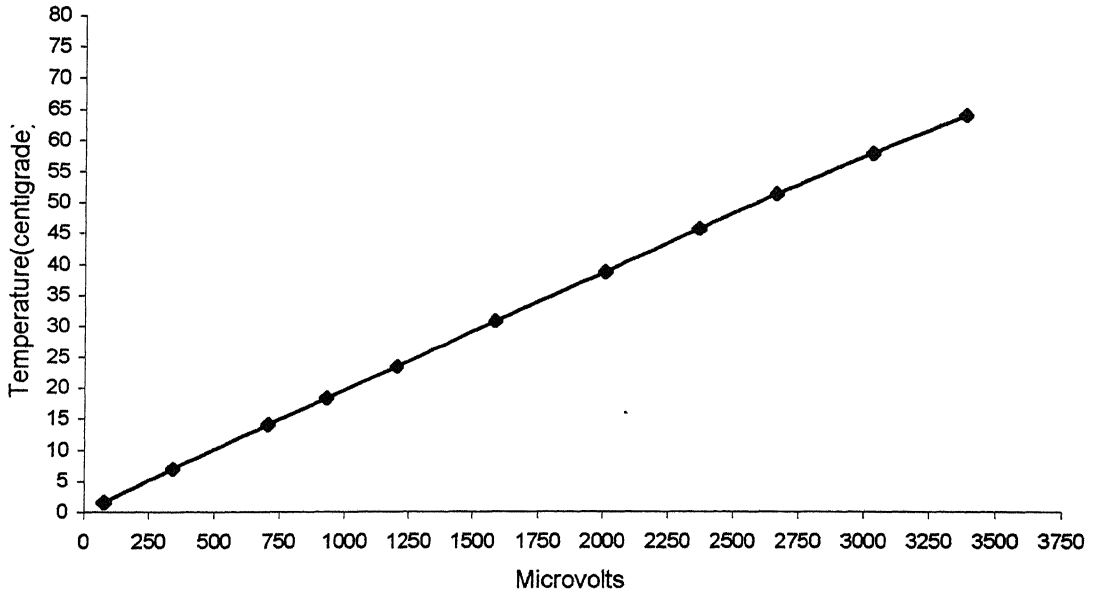

Figure 3.9 Calibration Chart for J type Thermocouple

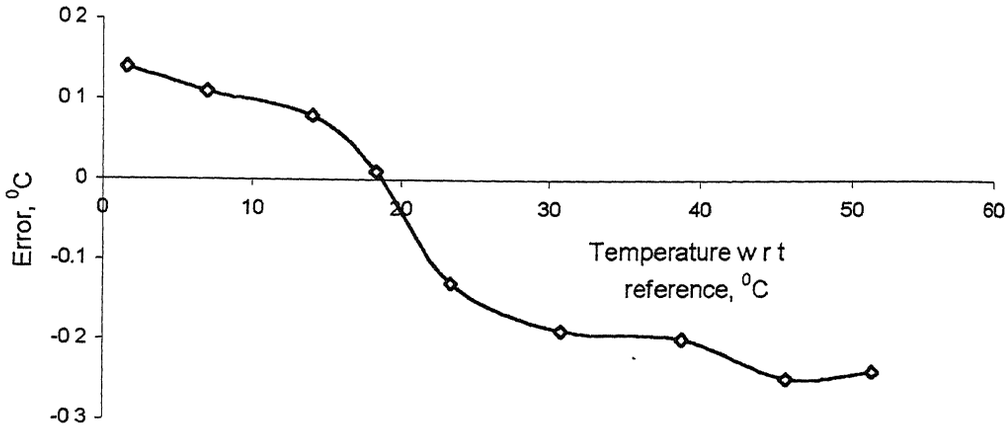

Figure 3.10 Error in Temperature measurement

3.5 Experimental Procedure

The experimental procedure adopted for the present study can be explained as follows: Before starting the experiment, the nozzle to plate separation distance is fixed at a particular separation distance. Subsequently the air is allowed to flow and its flow rate is adjusted with the help of nozzle flow meter in order to give a particular Reynolds number at the nozzle exit. The jet impingement is continued on the plate until (one hour) equilibrium state is reached. The adiabatic temperature readings at all data points are then recorded with the help of a precalibrated micro voltmeter. As explained earlier the use of adiabatic wall temperature results in a heat transfer coefficient that is independent of the wall heat flux. Nusselt number calculated by using this heat transfer coefficient is independent of the difference between the temperature of the jet and ambient temperature. Once the adiabatic temperature distribution is determined, the power supply to the test plate is turned on to generate a constant heat flux over its surface. The flow rate of the air jet is re-adjusted if some variation is observed. The system is again allowed for a considerable time (appox. two hours) to reach steady state. Then the outputs of all the thermocouples in the test plate again are recorded with the help of same micro-voltmeter. These millivolts values are subtracted from the corresponding values obtained

for adiabatic wall temperature measurements and subsequently converted into corresponding temperature with the help of calibration chart. The heat flux at the test plate is calculated from the measured current and voltage across the test plate. The local heat transfer coefficients at different locations of the test plate are calculated by the procedure given below.

As already defined the heat transfer coefficient may be given as,

$$h = \frac{q}{T_w - T_{aw}}$$

Where q = convective wall heat flux

T_w = Wall temperature measured in the presence of heating

T_{aw} = Adiabatic temperature measured in the absence of heating

With the help of heat transfer coefficient Nusselt number at different locations are calculated.

The local Nusselt number is defined as

$$Nu = \frac{hD}{k}$$

Where D = jet diameter

k = thermal conductivity of air at film temperature T_f which is given by

$$T_f = \frac{T_{w+} + T_\infty}{2}$$

3.5.1 Sample Calculation

Calculation for the Nusselt number at the stagnation point for Reynolds number 35,000 and H/D=6

Voltage across the test plate	= 13.72 volts
Current in the circuit	= 8.67 ampere
Area of the test plate	= 0.30 x 0.28 m^2
Jet diameter	= 7 mm.

Thermal conductivity of the air = 0.027 W/ m- K at 35 °C.

$$q = \frac{13.72x8.67}{0.30x0.28} = 1411 W/m^2$$

$$T_w - T_{aw} = 2.52^0 C$$

$$Nu = \frac{hD}{k} = \frac{561\ x.007}{0.026} = 151$$

$$h = \frac{q}{T_w - T_{aw}} = \frac{1416}{2.52} = 561\ .W\ /\ m^2$$

In this way Nusselt number at every data point is calculated and plotted against non-dimensional radial distance r/d. The whole procedure is repeated for different sets of Reynolds number and nozzle to plate separation distances and for various experimental models.

3.6 Experimental Precautions

During the experimental runs, the following precautions have been taken care of:

1. The test-plate is leveled in a horizontal position with the help of leveling screws.
2. Before every run the centerline of each model is aligned properly with the mid-point of the test plate where first thermocouple is located.
3. The settling chamber is kept in a vertical position to make the jet only in vertical direction.
4. Leakage test is performed before the experiment in order to make the set-up completely free with leakage even at high Reynolds numbers.
5. The air is maintained at same value of temperature for determination of T_w and T_{aw}.
6. The experimental setup is placed in a large room with a constant ambient temperature.
7. The system is allowed to reach steady state before every set of readings.

3.7 Validation of the experimental set-up

In order to validate the experimental set-up the heat transfer data obtained in the present study is compared with the similar data reported by Viskanta et al in 1996. The comparison between the two results is shown in the Figure 3.10. The comparison is made at Reynolds Number 20000 and nozzle to plate spacing of 6D. In both studies orifice jets are considered but the design of orifice in the two cases are found slightly different. The orifice in the current experiment has a diameter of 7 mm with length to diameter ratio of 0.44 whereas in the case mentioned the diameter is 12.7 mm with a L/D ratio of 1.5. The trends of the graphs plotted between the Nusselt number and non-dimensional radial distance for the two cases are found similar. It can be noted that the stagnation point Nusselt number in our experiment was found only 3.75% lower than the stagnation point Nusselt Number reported by Viskanta et al which is well within the uncertainty range. Moreover the instrumentation of the two experiments are different. Viskanta et al used liquid crystal technique for the measurement of temperature. However in the present study iron-constantan thermocouples are employed for the same. Therefore the validation results obtained are quite convincing and setup is working properly.

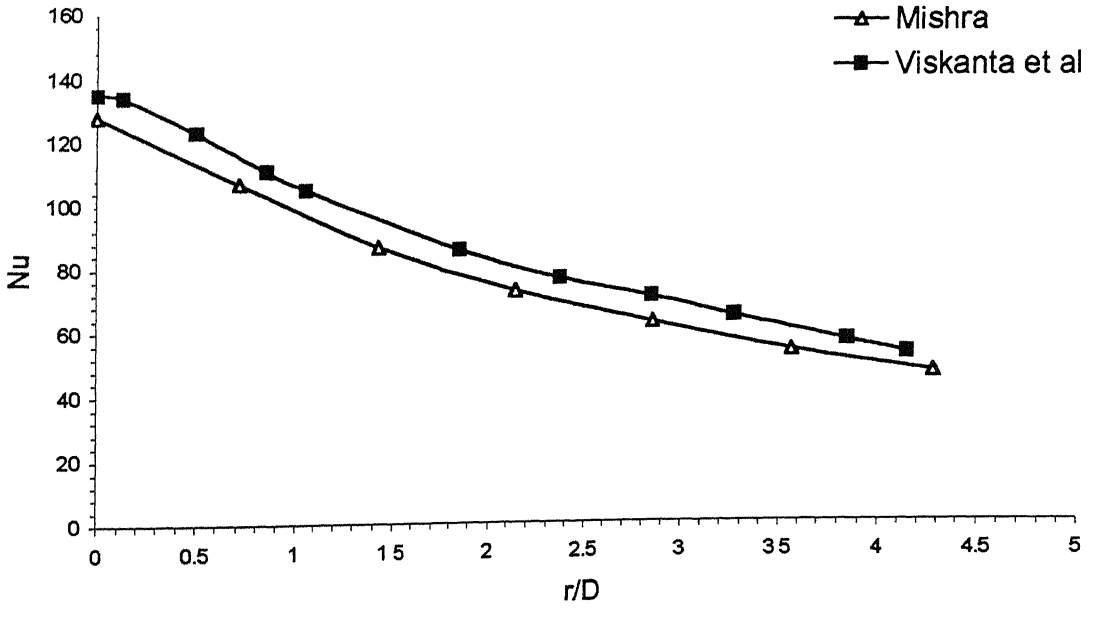

Figure 3.11 Validation of Experimental Set-Up

3.4 Concluding Remarks

In the present chapter the experimental set-up for the study of jet impingement cooling is discussed. Most of the fabrication work involved is carried out in the propulsion laboratory and departmental workshop. The experimental rig, various experimental models, nozzle flow meter, calibration unit for thermocouples and many small components like manometer, thermocouples etc have been fabricated in the process of development of experimental setup. The fabrication details of the experimental rig and measuring devices like nozzle flow meter are described in detail. The thermocouples, micro-voltmeter and nozzle flow meter are calibrated properly before taking measurements. The experiments are conducted with utmost care and first temperature distribution data for an orifice jet was recorded very carefully. The data obtained for the orifice is compared with the similar kind of data obtained by Viskanta et al. [1996]. The present results lie well within the experimental error limits with the data of Viskanta et al and are found in close agreement. After validating the experimental set-up extensive experimental study is carried out for various arrangements of different experimental models. The results obtained for these experiments are discussed in the next chapter in detail.

Chapter 4

RESULTS AND DISCUSSION

4.1 Introduction

While surveying the literature on jet impingement heat transfer it was revealed out that geometric factors associated with an impinging jet play a very vital role in determining its heat transfer characteristics. The main geometric factors which influence the heat transfer properties of impinging jets are the diameter of the jet nozzle, the nozzle-to-impingement surface spacing, the angle of incidence of jet axis and the design of the nozzle. Among the above geometric factors the design of nozzle is very important in determining the heat transfer properties of impinging jet. It is conjectured that the design of the nozzle affects the jet velocity profile at the jet exit. Thereby it influences the behavior of vortices around the jet circumference and the turbulence level generated in the shear layer. The variation in the level of turbulence caused by the alteration in nozzle design in turn affects the centerline jet velocity and so the length of the potential core. Therefore optimal nozzle to plate spacing for maximum heat transfer is determined by turbulence factor caused by the nozzle design and can be obtained by keeping these factors into consideration. Therefore, the present study has been aimed to investigate the effect of nozzle geometry on the cooling effectiveness of the impinging jets.

4.2 Present Study

In different industrial and engineering applications various types of nozzle configurations are employed. However, among them orifice is the most popularly used configuration because of its ease of fabrication and less space requirement for the installation. Therefore in the present studies a particular attention has been paid to the study of impinging jets ejecting from orifice jets. In order to investigate the heat transfer performance of orifice jets an extensive experimentation has been carried out on a square-edged orifice of 7 mm outlet diameter. The tests are conducted for Reynolds numbers 20000, 35000, 45000, 55000 and nozzle-to-plate spacing 4D, 6D, 8D and 10D.

Empirical correlations are also drawn relating the jet Reynolds number and nozzle-to-plate spacing with the stagnation Nusselt number.

Besides orifice the other popular jet configurations are nozzle and pipe. The jets ejecting from these configurations behave differently under different geometric circumstances. In order to make a proper selection and ascertain their optimum performance for a particular application it is needed to make a comparative study on them. During the course of literature survey it was revealed out that a little work has been devoted to investigate these comparative aspects of impinging jets. Hence, a study has been carried out in the present investigation among orifice, nozzle and pipe jets in order to ascertain their comparative performance.

An attempt for the heat transfer enhancement for orifice jet has also been made in the present work. The square-edged orifice used in the previous studies is replaced by an orifice, which is made sharp-edged by chamfering its outlet edge an angle of 60° to attempt enhancement in heat transfer. The experiments with the sharp-edged orifice are conducted for separation distances of 4D, 6D, 8D and 10D and Reynolds numbers 20000, 35000, 45000, and 55000. The average and stagnation Nu numbers are obtained for the sharp-edged orifice jet and compared with the corresponding values produced by square-edged orifice jet. These comparative values are presented in Table 4.4 and 4.5 for average and stagnation Nusselt numbers respectively. All the experiments are conducted with an uniform heat flux of 1400 W/m^2 over the surface of the test plate.

4.3 Results and Discussion

The results of present studies are reported in terms of variation of local Nusselt number (Nu) with the non-dimensional radial distance (r/D). At first the case of the orifice jet has been taken into consideration. The Nu vs. r/D plots for square-edged orifice at separation distance of 4D, 6D, 8D and 10D and Reynolds number 20000, 35000, 45000 and 55000 are presented in the Figure 4.1, 4.2, 4.3 and 4.4. It can be observed from the Figure 4.1 that the plots for different Reynolds number are fairly distinct up to a radial distance of 5D. Beyond this distance these plots tend to merge with each other, as the difference between them is not substantial. Therefore in the subsequent plots the variation of Nu number has been considered only up to radial distance of 5D.

It is observed from Figure 4.1 to 4.4 that maximum Nusselt number for all separation distance is found to occur at the respective stagnation points. The stagnation point Nusselt number for all separation distances and Reynolds numbers are presented in Table 4.1. It can be noted from the table that the maximum value of stagnation Nusselt number occurs at a separation distance of 6D for each Reynolds number. The subsequent highest values of stagnation point Nusselt number are obtained for separation distances of 4D, 8D and 10D respectively. It is also noted that the stagnation Nusselt number for separation distance of 4D is found to be higher than its value in the case of 8D separation distance. This may be explained by the fact that for orifice jets the length of the potential core extends up to the separation distance of 5D to 6D [Gauntner et al 1970]. Since jet velocity remains unchanged inside the potential core zone the jet velocity is expected to be substantial at this separation distance. At around same separation distance the intensity of turbulence attains its peak value [Gardon and Akfirat 1965]. Therefore the combined effect of high centerline velocity and peak turbulence level accelerates the heat transfer and maximum Nusselt number is obtained at the separation distance of 6D. Beyond the end of potential core the centerline velocity of the jet falls rapidly and as a result comparatively lower value of Nusselt number is obtained at 8D separation distance. However at separation distance of 4D the centerline velocity of the jet is substantial to produce higher Nusselt number in comparison to its value at 8D separation distance.

In Figure 4.1 to 4.4 Nu vs. r/D plots for orifice jet are presented for the separation distance of 6D, 4D, 8D and 10D respectively considering Reynolds number 20000, 35000, 45000 and 55000 for each separation distance. It is noticed that a general trend of high Nusselt number for high Reynolds number is obtained for all separation distances. The maximum values of the of stagnation as well as average Nusselt numbers is obtained at separation distance of 6D and 55000 Reynolds number. The stagnation and average Nusselt values for all the cases are presented in the Table 4.1. For Reynolds number 35000 the average Nusselt number at separation distance of 6D is higher than its values at 8D, 4D and 10D by 12.6%, 6%and 21.6% respectively.

The jet Reynolds number (Re) and nozzle-to-plate separation distance (H/D) are correlated to give stagnation point Nusselt number for the case of orifice jet. The correlation for the square-edged orifice is derived as

$$Nu_0 = 0.544\, Re^{0.553}(H/D)^{-0.081}$$

It is obvious from the relation that the stagnation point Nusselt number strongly depends upon Reynolds number in comparison to separation distance.

Re / H/D	20000 Stag. (Avg)	35000 Stag. (Avg.)	45000 Stag. (Avg.)	55000 Stag. (Avg.)
4	118(78)	151(104)	178(122)	210(149)
6	127(85)	161(112)	190(131)	224(158)
8	108(79)	141(99)	166(117)	196(142)
10	105(73)	132(89)	156(109)	183(131)

Table 4.1 Stagnation and average Nu for square-edged orifice

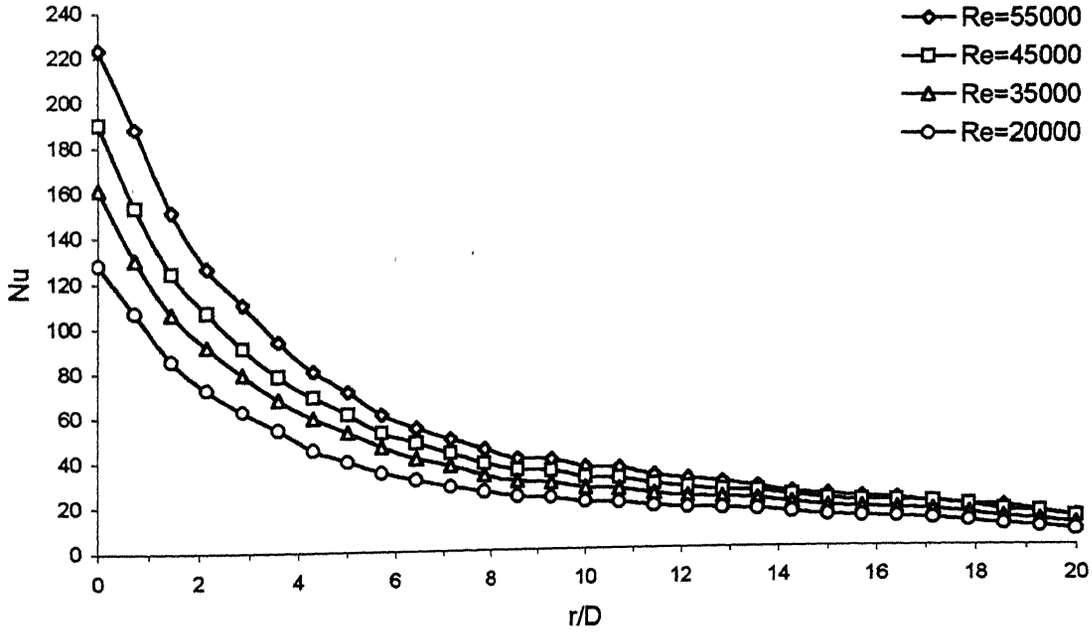

Figure 4.1 Local Nu distribution for square-edged orifice at H/D=6.

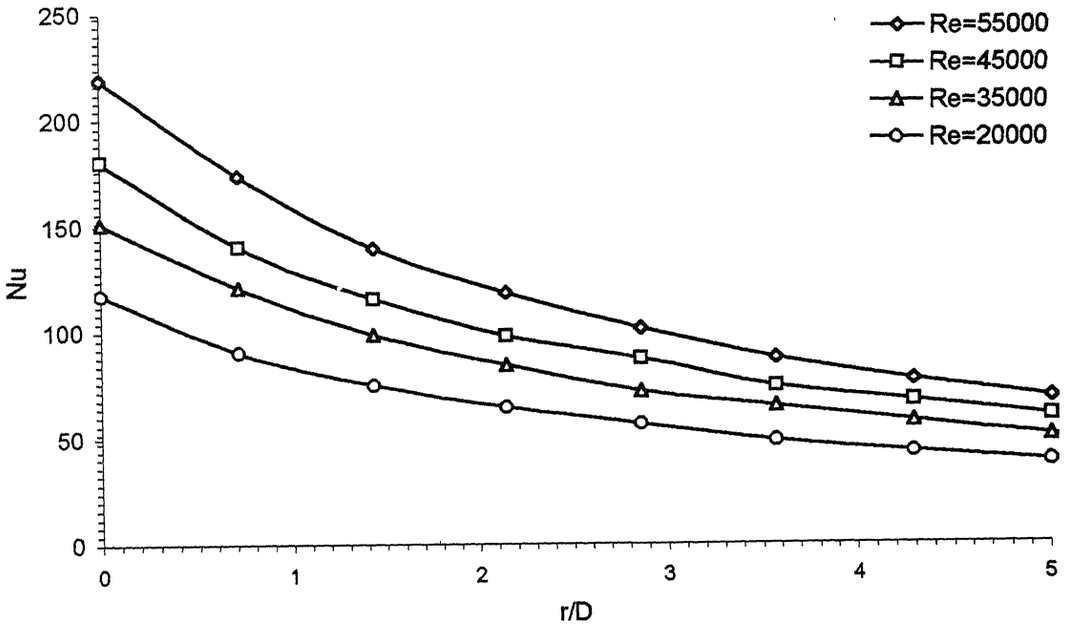

Figure 4.2 Local Nu distribution for square-edged orifice at H/D=4.

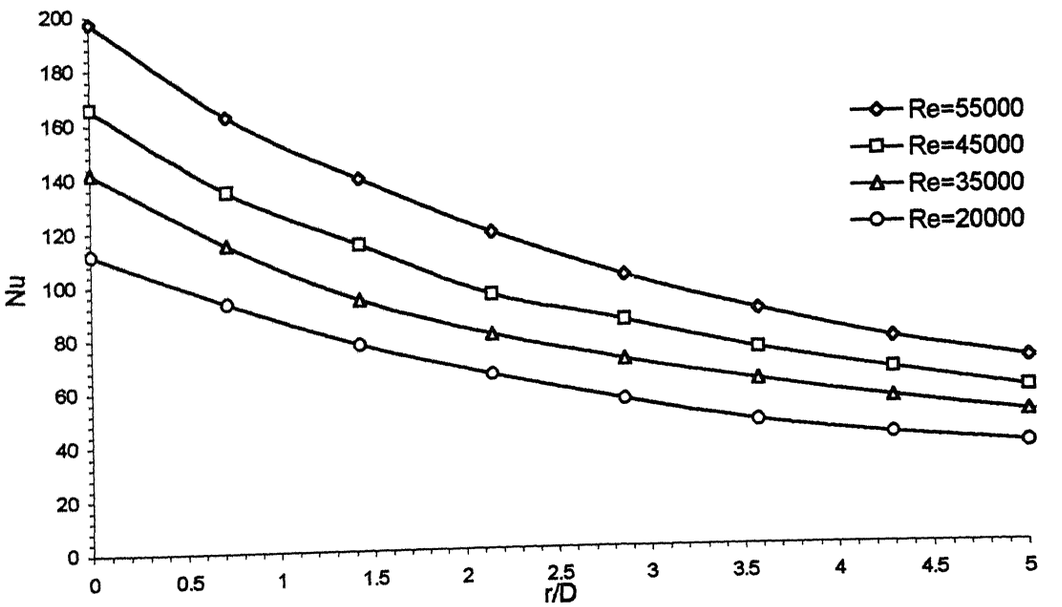

Figure 4.3 Local Nu distribution for square-edged orifice at H/D=8.

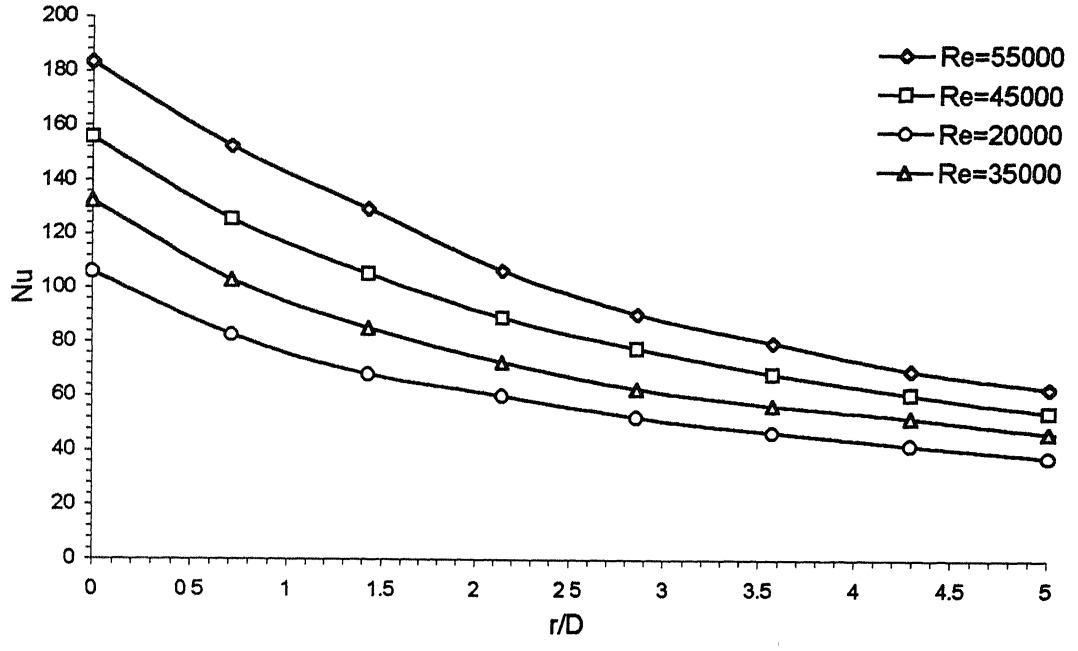

Figure 4.4 Local Nu distribution for square-edged orifice at H/D=10.

The heat transfer results for nozzle jet are presented in Figure 4.5 for the case of Reynolds number 35000. It is observed that the stagnation Nusselt number values for the separation distances of 4D, 6D, 8D and 10D are found to be 155, 138, 126 and 110 respectively. Interestingly the highest stagnation point Nusselt number for the nozzle jet is obtained at the separation distance of 8D, which is not the case for orifice jet. The subsequent highest values of stagnation Nusselt number are obtained for separation distances of 6D, 4D and 10D respectively. It can be explained by the fact that in the case of nozzle the initial level of turbulence in comparison to that of orifice jet may be quite low due to the smooth passing of air through the nozzle. In the case of nozzle jet the potential core is also longer due to the one-dimensional velocity profile of the jet at the exit. Therefore the transition of flow from laminar to turbulent state is expected to take place at a little longer separation distance in comparison to orifice jet and peak turbulence intensity may also expected to occur at longer separation distance. It may be due to these effects the maximum Nusselt number is found to occur at the separation distance of 8D with the subsequent higher values occurring at separation distances of 6D, 4D and 10D respectively.

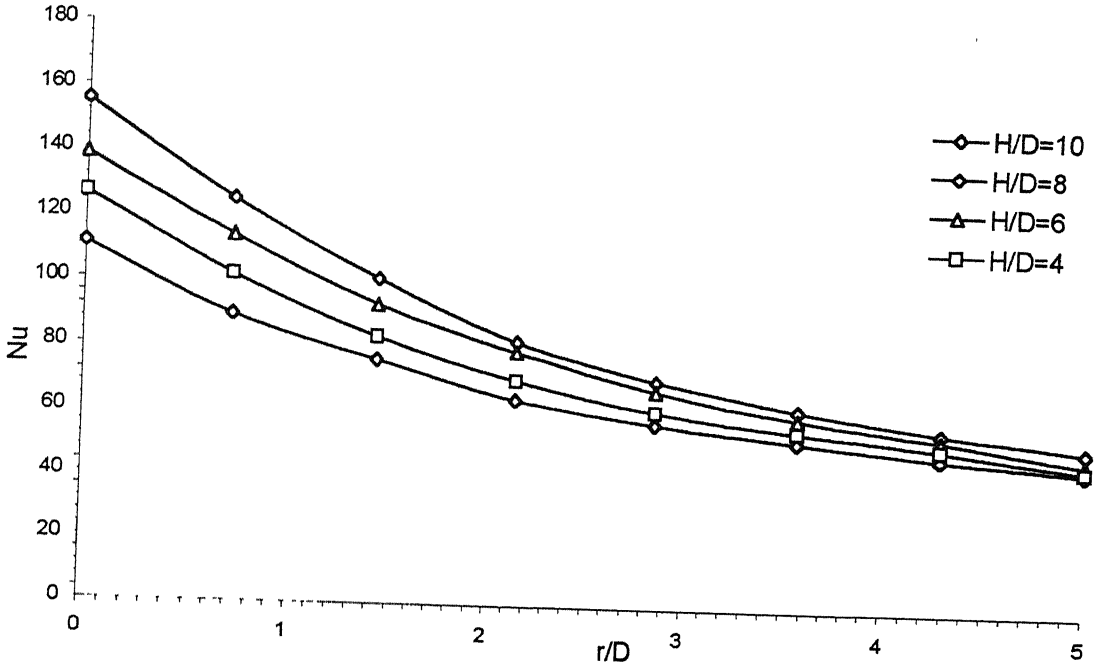

Figure 4.5 Local Nu distribution for a nozzle jet at Re=35000.

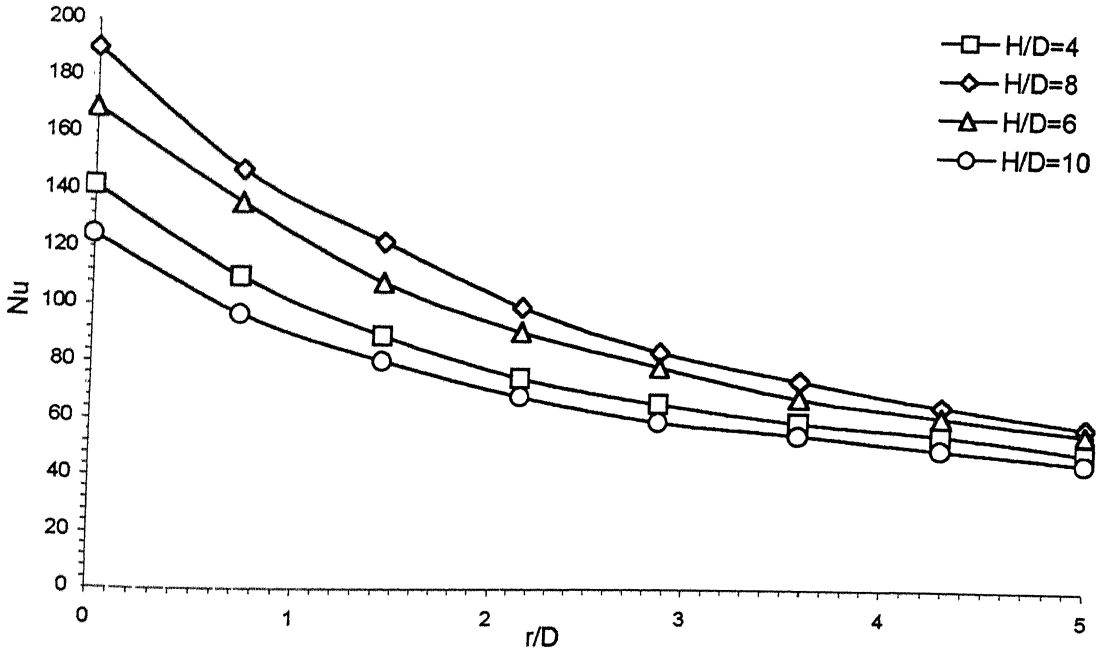

Figure 4.6 Local Nu distribution for a pipe jet at Re=35000.

The heat transfer results for a pipe jet are presented in Figure 4.6 for Reynolds number 35000. The plots show the stagnation Nusselt numbers of 190, 168, 142 and 124 for separation distances of 8D, 6D, 4D and 10D respectively. It is noteworthy that the maximum stagnation Nusselt number is obtained at separation distance of 8D as in the case of nozzle jet. The subsequent higher values of stagnation Nusselt number are found at separation distances of 6D, 4D and 10D respectively. The reason might be that for pipe jets the flow at the exit is fully developed which increases the length of the potential core and intensifies the turbulence level at longer separation distance. Probably due to these effects the maximum heat transfer for pipe jets is obtained at separation distance of 8D with the subsequent higher values at 6D, 4D and 10D respectively. However, the above observation is based on mere conjecture, and requires detailed investigation.

In order to see the comparative performance of orifice, nozzle and pipe jets combined plots for the three configurations at separation distances of 4D, 6D, 8D and 10D are presented in Figure 4.7, 4.8, 4.9 and 4.10 respectively. It can be observed from these plots that the orifice jets produce maximum heat transfer at separation distance of 6D. The subsequent higher values of heat transfer are obtained at separation distance of 6D, 4D and 10D respectively. For both nozzle and pipe jets the highest stagnation Nusselt numbers is obtained at separation distance of 8D with the subsequent higher values at separation distances of 6D, 4D and 10D respectively. The average and stagnation Nusselt numbers for the three configurations are presented in Table 4.2 and 4.3 respectively. The percentage change in the values of Nusselt number in comparison to the least corresponding value produced by a configuration is also presented within parenthesis. The increment is found to be maximum for separation distance of 8D in the case of pipe jet.

For the whole experimentation the maximum uncertainty level is maintained in the range of 6-7%. The largest contributor to this is the uncertainty in the measurement of temperature. A maximum uncertainty of 5% is encountered in the determination of stagnation point temperature. The uncertainties in the Reynolds number calculation and heat flux determination on the test plate are estimated to be less than 4% and 2.5% respectively.

H/D	Nozzle (% increase*)	Pipe (% increase*)	Orifice (% increase*)
4	87	94 (8)	104 (16.3)
6	97	114 (17.5)	112 (15.46)
8	105 (6.06)	127 (20.9)	99
10	78	85 (8.9)	89 (14.1)

*w.r.t. to the least corresponding value

Table 4.2 Average Nu for orifice, nozzle and pipe jets at Re=35000.

H/D	Nozzle (% increase*)	Pipe (% increase*)	Orifice (% increase*)
4	126	142 (12.6)	151(19.8)
6	138	168 (21.7)	161(16.66)
8	155 (9.15)	190 (33.8)	142
10	110	124 (12.7)	132(20)

*w.r.t. to the least corresponding value

Table 4.3 Stagnation Nu for orifice, nozzle and pipe jets at Re=35000.

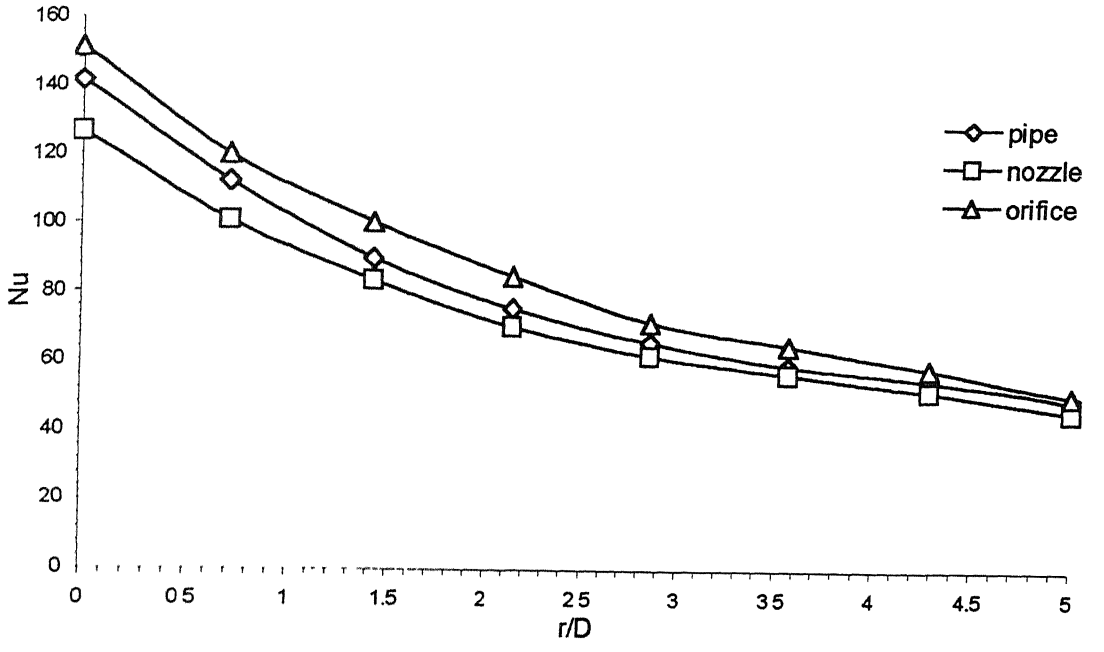

Figure 4.7 Local Nu distribution for orifice, nozzle and pipe jets at H/D=4.

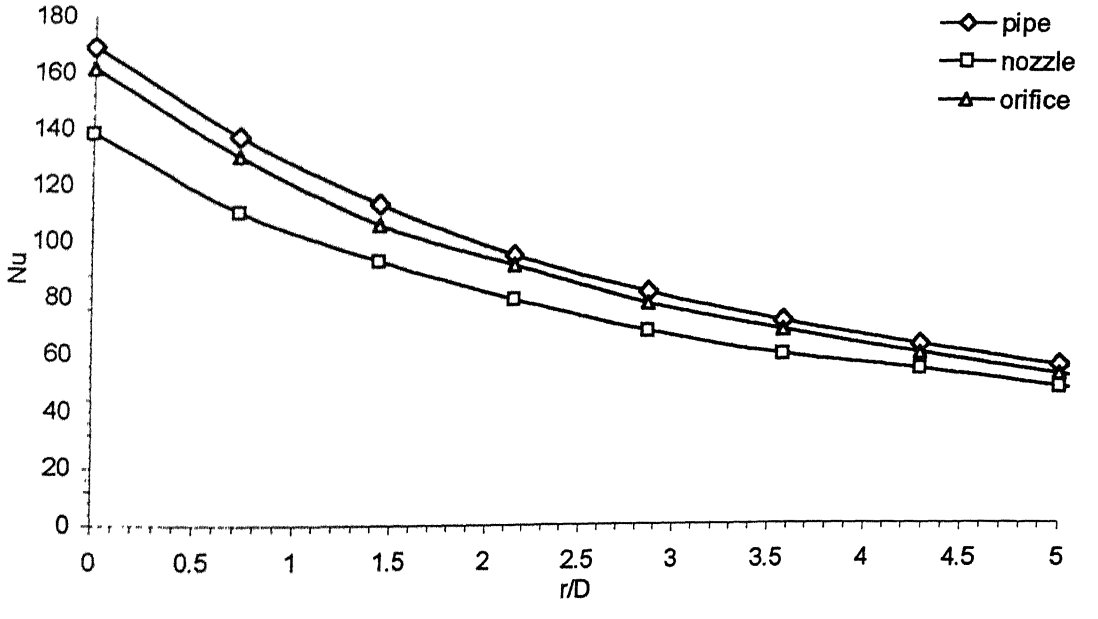

Figure 4.8 Local Nu distribution for orifice, nozzle and pipe jet at H/D=6.

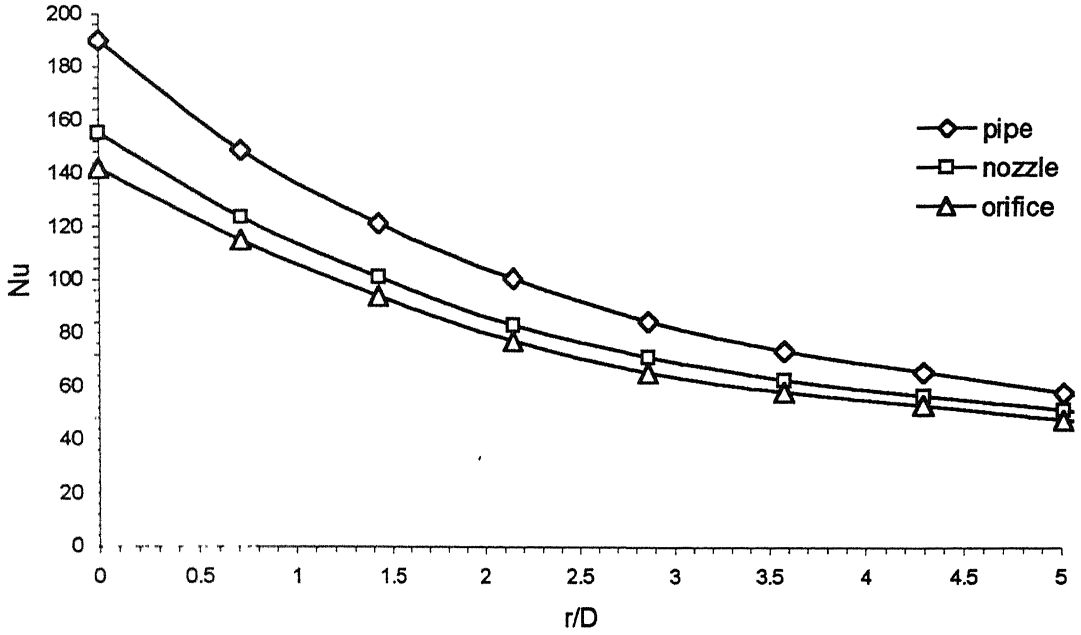

Figure 4.9 Local Nu distribution for orifice, nozzle and pipe jet at H/D=8.

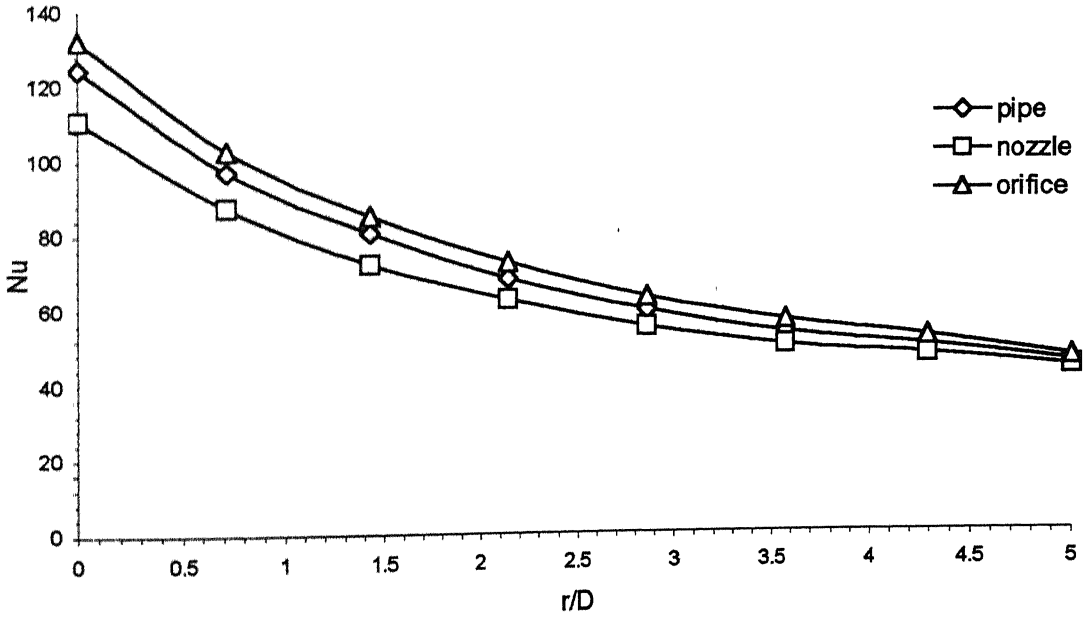

Figure 4.10 Local Nu distribution for orifice, nozzle and pipe at H/D=10.

4.4 Enhancement of Impingement Cooling

In this section the enhancement in heat transfer by a jet ejecting from an orifice jet has been attempted. During literature survey it was observed that the heat transfer to an impinging jet is affected by the initial level of turbulence present at the nozzle exit [Hoogendoorn 1971]. This effect is found to be pronounced for separation distance less than 6D. For separation distance greater than 6D, the turbulence generated in the shear layer predominates [Gardon and Akfirat 1965]. The initial level of turbulence is expected to be associated with the geometry of the jet configuration employed. The level of turbulence may be low if the jet is ejecting from a well- designed contoured nozzle. However the level of turbulence is expected to be higher if the jet is ejected through a sharp-edged orifice. This turbulence present at the nozzle exit might be affecting the behavior of vortices known as toroidal vortices around jet circumference. These toroidal vortices are convected to the impingement plate and in turn may increase the heat transfer from it. Orifice jets because of their abundant use and kinship to the gas turbine application are considered very important and are therefore chosen for enhancement studies in the present work.

The orifice employed in the present study is a sharp-edged orifice as shown in the Figure 3.3. In many respect it is similar to the square-edged orifice employed in the previous study. However its outlet edge is made sharp by chamfering it at an angle of 60^0. This outlet diameter of the orifice is kept at 7 ± 0.01 mm equal to square-edged orifice. While mounting the orifice on the settling chamber, care is taken to keep its chamfered face in the downward direction so that its functioning like a nozzle can be avoided.

Initially, the orifice jet is tested for Reynolds numbers 35000 and 55000 at nozzle-to-plate separation distance of 6D to check whether there is any enhancement or not. It is observed that enhancement of 11.6% and 18.9% in w.r.t. corresponding average Nusselt values for square-edged orifice is obtained for Reynolds number 35000 and 55000 respectively. Thereafter an extensive experimentation is carried out with the sharp-edged orifice at separation distances of 4D, 6D, 8D and 10D considering all Reynolds number 20000, 35000, 45000 and 55000 for each separation distance.

4.4.1 Results of Enhancement Heat Transfer

The results obtained for the enhancement studies are presented in figures 4.11,4.12, 4.13 and 4 14. Similar to the case of square-edged orifice, in the present case too the peak stagnation Nusselt numbers are found to occur at the separation distance of 6D for all Reynolds number cases. The stagnation values for all Reynolds number and separation distances are presented in Table 4.5. In order to calculate the average Nusselt numbers, local values of Nusselt number are averaged up radial distance of 5D using trapezoidal rule for the integration. These averaged results are compared with the corresponding values obtained for square edged orifice. The average Nu values for both the orifices are presented in the Table 4.4. It is obvious from this table that significant enhancement is obtained in the case of Reynolds number 55000 and 45000 at H/D =6 and 4. However for higher H/D and lower Reynolds number the enhancement is found to be just marginal. The maximum enhancement of 18.9% in average Nu is obtained at Re=55000 and separation distance of 6D. Since the turbulent level is expected to be higher between separation distance of 4D to 6D, the enhancement in the heat transfer coefficient is expected. But as the separation distance increases, the turbulence intensity falls rapidly and the enhancement effect diminishes.

For sharp-edged orifice too, jet Reynolds number (Re) and nozzle-to-plate spacing (H/D) have been correlated to give the stagnation Nusselt number Nu_0 as

$$Nu_0 = 0.561\ Re^{0.575}(H/D)^{-0.113}$$

It is noticed that the values of index and the constant is higher than the corresponding values for the square-edged orifice. Therefore sharp-edged orifice is more suitable for the enhancement of heat transfer.

Re / H/D	20000	35000	45000	55000
4	89(78)	118(104)	139(122)	169(149)
6	92(85)	125(112)	153(131)	188(158)
8	88(79)	111(99)	129(117)	153(142)
10	80(73)	99(89)	116(109)	140(131)

Table 4.4 Average Nu for square and sharp edged orifices.

Re / H/D	20000	35000	45000	55000
4	138(118)	181(151)	215(178)	255(210)
6	153(127)	194(161)	230(190)	272(224)
8	131(111)	169(141)	201(166)	238(196)
10	126(105)	159(132)	188(156)	222(183)

Table 4.5 Stagnation Nu for sharp and square-edged orifices.

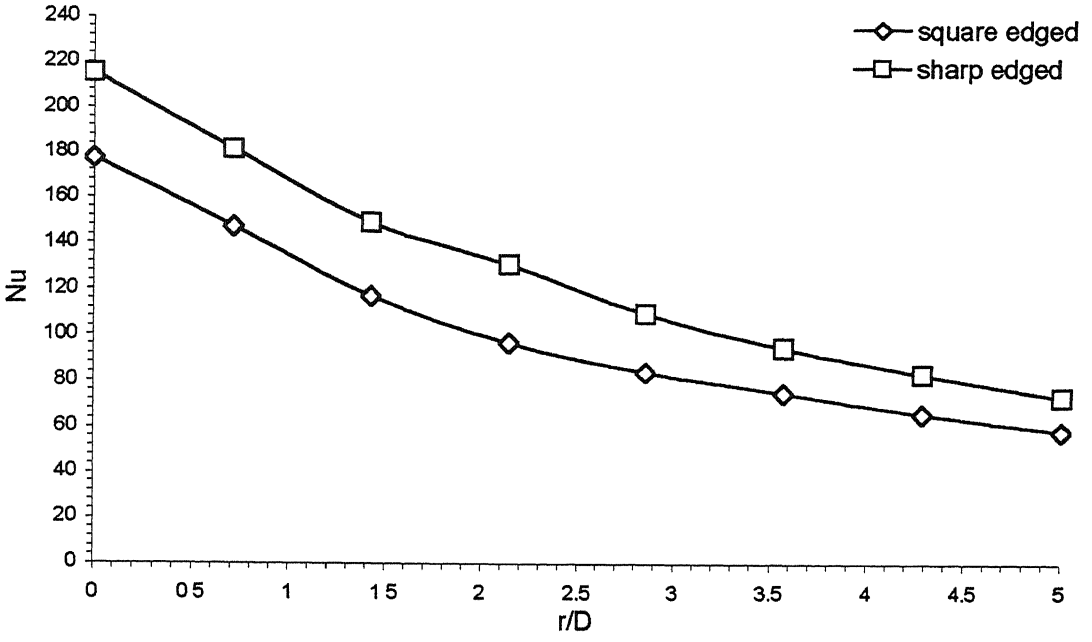

Figure 4.11 Comparison between two orifices at H/D =4 and Re=55000.

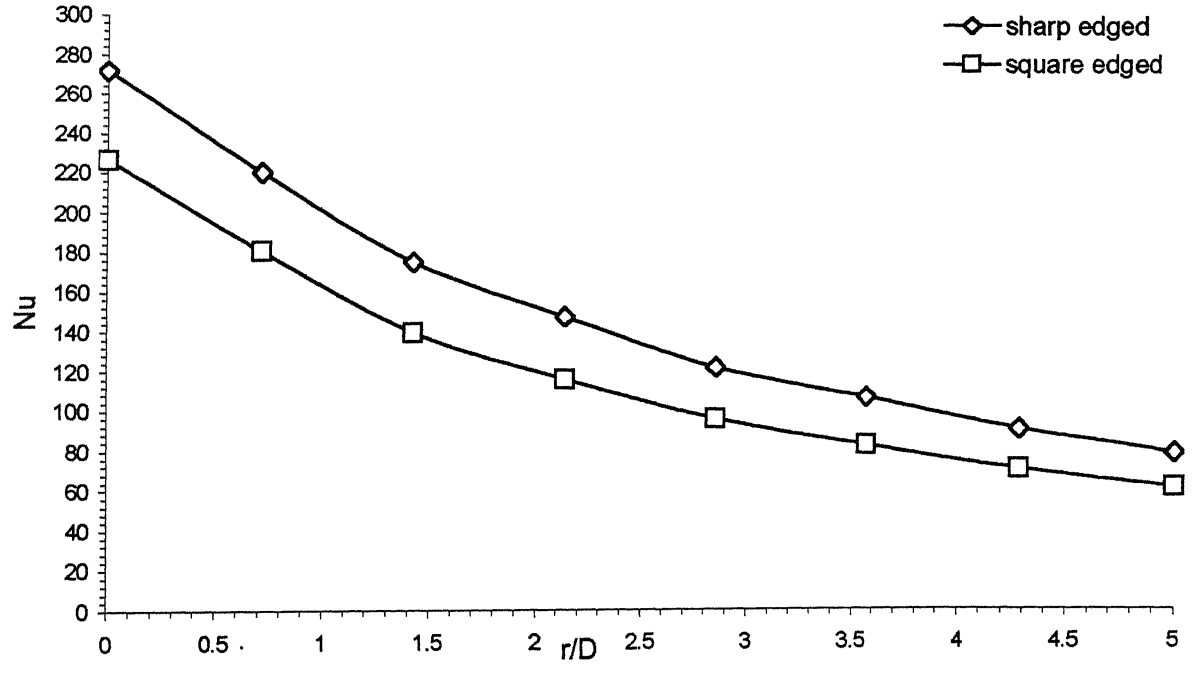

Figure 4.12 Comparison between two orifices at H/D =6 and Re=55000.

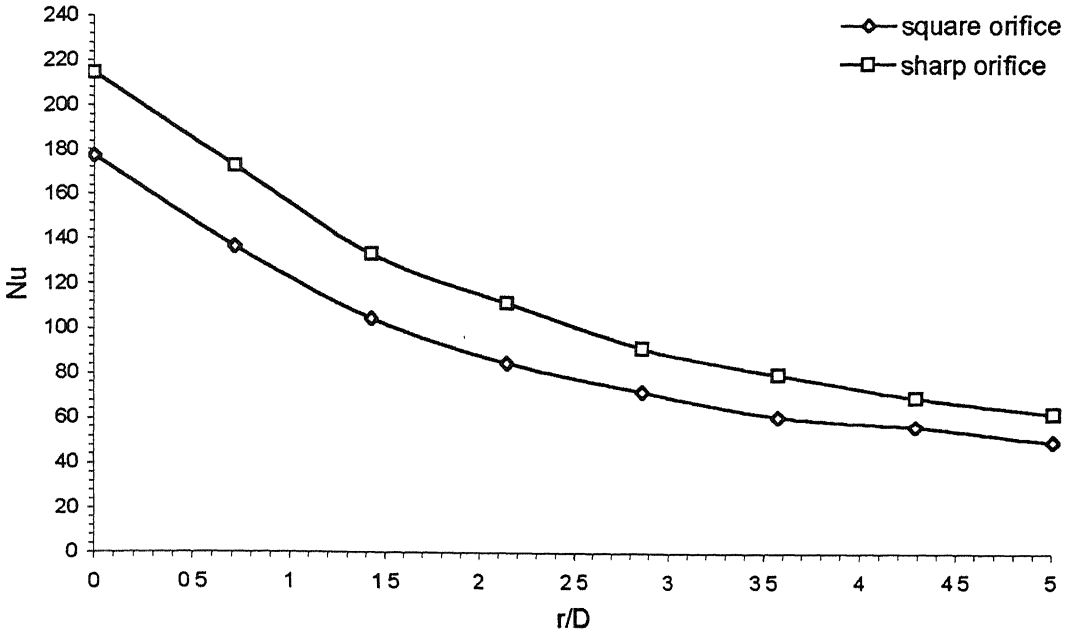

Figure 4.13 Comparison between two orifices at H/D =4 and Re=45000

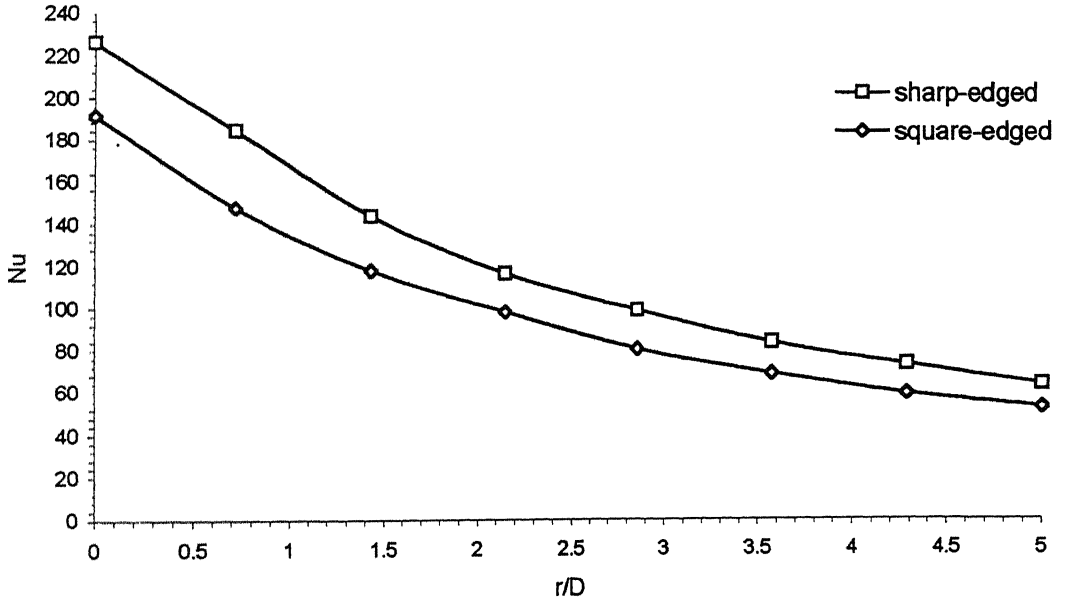

Figure 4.14 Comparison between two orifices at H/D =6 and Re=45000

4.5 Summary and Conclusions

In the present studies, an experimental investigation of convective heat transfer to round impinging jets from a flat plate at various Reynolds number and H/D ratios has been carried out. In order to conduct the present investigation, a complete experimental rig equipped with a test-plate, jet facility, and electrical accessories has been design and developed in our laboratory. Three types of experimental models namely orifice, convergent nozzle and pipe jets have been employed for the investigation. However, the main emphasis is given to the study of orifice jets because of their wide-ranging applications and kinship to gas turbine cooling. Experiments for orifice are conducted for Reynolds number 20000, 35000, 45000 and 55000 and nozzle-to-plate separation distance of 4D, 6D, 8D and 10D. Orifice jets are found to show maximum stagnation point Nu number at separation distance of 6D for the whole range of Reynolds number. The subsequent highest stagnation point Nu numbers are obtained for separation distances of 4D, 8D and 10D respectively. The stagnation Nu number increases with the increase in Reynolds number and for Reynolds number 55000, 45000 and 35000, respective percentage increase of 82%, 42% and 20.4% are obtained in comparison to its value at Re=20000 for H/D=6. The average values of Nu number are calculated from local values and for separation distance of 6D these are found to be 188, 153, 125 and 92 for Reynolds number 55000, 45000, 35000 and 20000 respectively.

The effect of nozzle geometry on the heat transfer characteristics of the impinging jets has also been investigated at Reynolds number of 35000. In this regard a comparative study of three experimental models namely orifice, nozzle and pipe is conducted for the separation distances of 4D, 6D, 8D and 10D. The maximum stagnation Nusselt numbers for orifice, nozzle and pipe jets are found to be 161, 151 and 190 respectively at the separation distances of 6, 8 and 8. The minimum stagnation Nu number is obtained at H/D=10 for all three types of models. For orifice jets, heat transfer at separation distance of 4D is higher than that obtained for the separation distance of 8D. In the contrast, a pipe jet shows more heat transfer at 8D separation distance than separation distance of 4D. Similar to the pipe, the nozzle jet also has higher heat transfer coefficient at separation distance of 8D in comparison that at separation distance of 4D. Therefore it

may concluded that pipe and nozzle are suitable for higher H/D values whereas orifice jets should be preferred for smaller H/D ratios.

The enhancement in the case of orifice is also attempted by replacing square edged orifice with a sharp-edged orifice. The stagnation and average values of Nu at H/D=4, 6, 8 and 10 and Re= 20000, 35000, 45000 and 55000 are obtained for sharp-edged orifice and compared with the corresponding values obtained for square-edged orifice. The percentage increment in heat transfer is calculated for each case. The maximum enhancement of 18.9% in average Nusselt number is obtained for Reynolds number 55000 and separation distance of 6D However the enhancement is just 8.2% at same separation distance and Reynolds number 20000. It implies that enhancement effect is more pronounced at higher Reynolds number. It is also noticed that at Reynolds number of 55000 the percentage increments in heat transfer for separation distances of 6D and 4D are18 9% and 13 4% respectively However for separation distances of 8D and 10D the percentage increments are found to be just 7.7% and 6.8%. Therefore, it can be concluded that enhancement effect is pronounced for smaller separation distances separation distance in the range of 4D to 6D.

The correlations for the two orifices are also derived and can be presented as

$$Nu_0 = 0.544\, Re^{0.553}(H/D)^{-0.081} \quad - \quad \text{Square-edged orifice}$$

$$Nu_0 = 0.561\, Re^{0.575}(H/D)^{-0.113} \quad - \quad \text{Sharp-edged orifice}$$

It is obvious from the above two relations that the indices for separation distance and Reynolds number for the sharp-edged orifice are higher than its value for square-edged orifice. Thus sharp-edged orifice is more suitable for the enhancement of heat transfer at the stagnation point.

4.6 Suggestion for Future Work

The following experimental work may be suggested for future studies:

1. Suitable flow visualization technique can be employed in order to understand the nature of the impinging jets.
2. Three configurations of jet can be compared at higher Reynolds number.
3. Hot-wire measurements can be made for the determination of turbulence level and jet velocity profile at different H/D ratios.
4. Orifice with other geometrical shapes can be tested for the enhancement studies.
5. Enhancement of cooling can be attempted by large-scale eddy structures generated by the insertion of small circular cylinders in jet stream.

REFERENCES

Abramovich, G. N., *The Theory of Turbulent jets, MIT Press, Cambridge, Mass.*, (1963).

Bouchez, J. P., and Goldstein, Impingement Cooling from a Circular Jet in a Cross Flow, *International Journal of Heat Mass transfer* 18, 719-730 (1975).

Donaldson, C.D., Snedeker, R. S. and Margolis, D. P., "A Study of Free et Impingement, Part 1. Mean Properties of Free and Impinging Jets", *Journal of Fluid Mechanics* 45 (2), 281, (1971).

Donaldson, C.D., Snedeker, R. S. and. Margolis, D. P, "A Study of Free Jet Impingement: Part 2. Free Jet Turbulent Structure and Impingement Heat Transfer", *Journal of Fluid Mechanics* 45, 477-512, (1971).

Friedman, S. J. and Mueller, A. C., "Heat Transfer Between a Flat Plate and Jets of Air Impinging on it", *The Institute of Mechanical Engineers. London*, pp. 138-142 (1951).

Gardon, R. and Akfirat, J.C., "The Role of Turbulence in Determining the Heat-transfer Characteristics of Impinging Jets", *International Journal of Heat and Mass Transfer* 8, 1261-1272, (1965).

Giralt, F., Chia, C. J. and Trass, O., "Characterization of the impingement region in an axisymmmetric turbulent jet", *Industrial Engineering Chemistry Fundamentals*, 16, 21-28, (1977).

Glaser, H., *Chem. Ing. Tech.*34, 200 (1962).

Glauert, M. B., *Journal of Fluid Mechanics*, 1, 625-643, (1956).

Goldstein, R.J., Sobolik K.A. and Seol W.S., "Effect of Entrainment on the Heat Transfer to a Heated Circular Air Jet Impinging on a Flat Surface", *Journal of Heat Transfer 112*, 608-611 (1990).

Gordon, R. and Akfirat, J.C., "Heat Transfer Characteristics of Impinging Two-dimensional Air Jets", *Journal of. Heat Transfer* 88C(1), 101 (1966).

Gordon, R. and Cobonpue, J. "Heat Transfer Between a Flat Plate Jets of Air Impinging on it", *International Development in Heat Transfer, Proceedings of the 2nd International Heat Transfer Conference*, p. 454 *ASME, New York*, (1962).

Hoogendoorn, C.J., "The Effect of Turbulence on Heat Transfer at a Stagnation Point", *International Journal of Heat and Mass Transfer* 20, 1333-1338 (1977).

Jambunathan, K, Lai E., Moss M. A. and Button B. L., "A Review of Heat Transfer Data for Single Circular Jet Impingement", *International Journal of Heat and Fluid Flow*, Vol. 13, No.2, June, (1992).

Katoaka, K., "Impingement Heat Transfer Augmentation Due to Large Scale Eddies, *Heat Transfer* 1990", 1, 255-273, (1990).

Katoaka, K., Suguro, M.,Degawa.H., Maruo, K. and Mihata, I., "The Effect of Surface Renewal Due to Large Scale Eddies on Jet Impingement Heat Transfer", *International Journal of Heat and Mass Transfer*, 30, 559-567, (1987).

Livingood, N. B., Hrycak, P. and Gauntner, J. W., Survey of Literature on Flow Characteristics of a Single Turbulent Jet Impinging on a Flat Plate, *NASA TN D-5652* (1970).

Martin, H., "Heat and Mass Transfer Between Impinging Gas Jets and Solid Surfaces", *In Advances in Heat Transfer*, Vol. 13, pp. 1-60. *Academic Press, New York*, (1977).

Obot, N. T., Mujumdar, A.S. and Douglas, W. J. M., "Effect of Nozzle Geometry on Impingement Heat Transfer under a Round Turbulent Jet". *ASME Paper 79-WA/HF-53*, (1979b).

Perry, K. P., "Heat Transfer by Convection from a Hot Gas Jet To a Plane Surface", *Proceedings of Institution of Mechanical Engineers (London)*, 168 775-784, (1954).

Polat, S., Huang, B., Majumdar, A.S. and Douglas, W. J. M., Numerical Flow and Heat Transfer Under Impinging Jets: A Review, *Annual Rev. Num. Fluid Mech. Heat Transfer*, 2,157-197, (1989).

Popiel, C. O., and Trass, O., "Visualization of Free and Impinging Round Jets", *Experimental and Thermal fluid Science*, 4, 253-261, (1991).

Popiel, C.V., and Boguszawski, L., "Mass Transfer in Impinging Single, Round Jets Emitted by a Bell-Shaped Nozzle and Sharp-Edged Orifice", *Heat Transfer* 1986, 3, 1187-1192, (1986).

Schlunder, E. U. and Gnielinski. V., "Heat and Mass Transfer Between Surfaces and Impinging Jets", *Chem. Ing. Tech.*, 39. 578-584 (1967).

Scholtz, M. T. and O. Trass, "Stagnation Flow-Velocity and Pressure distribution", *Part A.I.Ch.E* 161, 82-90, (1970).

Sparrow, E., M., and Lee, L., "Analysis of Flow Field and Impingement Heat/Mass Transfer Due to a Nonuniform Slot Jet", *Journal of Heat Transfer*, 97, 191-197. (1975).

Vickers, J.M.F., "Heat Transfer Coefficients Between Fluid Jets and Normal Surfaces", *Journal of Industrial Engineering. Chemistry* 51, 967, (1959).

Viskanta R., "Heat Transfer to Impinging Isothermal Gas and Flame Jets", *Experimental Thermal and Fluid Science* 6, 111-134, 1993.

Viskanta, R. and Colucci D.W., "Enhancement of Local and Average Heat Transfer to a Confined Impinging Air Jet Using Hyperbolic Nozzles", *The Ninth International Symposium on Transport Phenomena in Thermal-Fluids Engineering, Singapore,* June 25-28, 1996.

Yokobori, S., Kasagi, N., Hirata M., Nakamaru, M. and Haramura,Y. "Characteristics Behaviour of Turbulence and Transport Phenomena at the Stagnation Region of an Axi-symmetrical Impinging Jet", *Proceeding of 2nd symposium on Turbulent Shear Flows, London, UK*, 4, 4.12-4.17 (1978)

Date Slip

The book is to be returned on the date last stamped.

.....	.....
.....	.....
.....	.....
.....	.....
.....	.....
.....	.....
.....	.....
.....	.....
.....	.....
.....	.....
.....	.....